

Washington University in St. Louis

Washington University Open Scholarship

McKelvey School of Engineering Theses & Dissertations

McKelvey School of Engineering

Spring 5-18-2018

An Evaluation of Proposed and Current Cardiovascular Stent Design Approaches to Aortoiliac Occlusive Disease

Alexander Wirtz

Washington University in St. Louis

Follow this and additional works at: https://openscholarship.wustl.edu/eng_etds



Part of the [Engineering Commons](#)

Recommended Citation

Wirtz, Alexander, "An Evaluation of Proposed and Current Cardiovascular Stent Design Approaches to Aortoiliac Occlusive Disease" (2018). *McKelvey School of Engineering Theses & Dissertations*. 342. https://openscholarship.wustl.edu/eng_etds/342

This Thesis is brought to you for free and open access by the McKelvey School of Engineering at Washington University Open Scholarship. It has been accepted for inclusion in McKelvey School of Engineering Theses & Dissertations by an authorized administrator of Washington University Open Scholarship. For more information, please contact digital@wumail.wustl.edu.

WASHINGTON UNIVERSITY IN ST. LOUIS
School of Engineering and Applied Science
Department of Mechanical Engineering and Materials Science

Thesis Examination Committee:
Dr. Mohamed Zayed, Chair
Dr. Guy Genin
Dr. Damena Agonafer

An Evaluation of Proposed and Current Cardiovascular
Stent Design Approaches to Aortoiliac Occlusive Disease

by
Alexander Joseph Wirtz

A thesis presented to the School of Engineering
of Washington University in St. Louis in partial fulfillment of the
requirements for the degree of
Master of Science in Mechanical Engineering

May 2018

Saint Louis, Missouri, USA

Contents

List of Figures	iv
List of Tables.....	vi
Acknowledgments.....	vii
Dedication.....	viii
Abstract	ix
1 Background.....	1
1.1 Aortoiliac Occlusive Disease.....	1
1.2 Current Treatment Solutions	3
1.3 Discussion of Proposed Design	7
1.3.1 Device Introduction.....	7
1.3.2 Model and Description of Device	8
1.4 Overview of Thesis.....	10
2 Methods	11
2.1 Models for the Aortic Bifurcation.....	11
2.2 Boundary Conditions and Assumptions.....	16
2.3 Discretization.....	17
2.4 Software.....	18
2.4.1 Solidworks	18
2.4.2 ANSYS Fluent	19
2.5 Experimental Parameters.....	19
2.6 Parametric Studies.....	21
3 Convergence Studies	22
4 Results	23
4.1 Healthy Bifurcation.....	23
4.2 Unhealthy Bifurcation	25
4.3 Kissing Stents	26
4.4 Proposed AIFEN Stent, 5mm Fenestration.....	29
4.5 Proposed AIFEN Stent, 10mm Fenestration.....	31
4.6 Proposed AIFEN Stent, 15mm Fenestration.....	34
4.7 Tabulated Data.....	36

5	Discussion	38
5.1	Mass Flow Rate	38
5.2	Average Outlet Velocity	39
5.3	Velocity Contour and Vector Plots	41
5.4	Vorticity	45
6	Conclusion and Future Work	47
6.1	Summary of Results	47
6.2	Future Work	48
Appendix	MATLAB Description of Inlet Blood Pumping	49
References		50
Vita		53

List of Figures

Figure 1.1:	Schematic of the aortic bifurcation cross-section with aortoiliac occlusive disease.....	2
Figure 1.2:	Schematic of the aortic bifurcation with placed kissing stents	4
Figure 1.3:	Schematic of the various cross-sections found at the inlet of the kissing stents procedure.....	5
Figure 1.4:	CT scan showing the presence of kissing stents in the distal aorta	6
Figure 1.5:	Schematic of the aortic bifurcation with the ipsilateral main Body aortoiliac stent design in place	8
Figure 1.6:	Schematic of the fenestrated stent design with labeled features	9
Figure 1.7:	Initial prototype concept for the fenestrated stent.....	10
Figure 2.1:	Image of the CAD cross-sections of the healthy aortic bifurcation model and the unhealthy aortic bifurcation model	12
Figure 2.2:	Image of CAD cross-section of the aortic bifurcation model with placed kissing stents	13
Figure 2.3:	Image of CAD wireframe view of the aortic bifurcation model with placed kissing stents	13
Figure 2.4:	Image of CAD cross-section of the aortic bifurcation model with the fenestrated stent designs.....	15
Figure 2.5:	Image of CAD wireframe view of the aortic bifurcation model with the proposed AIFEN stent design	15
Figure 2.6:	Plot of the blood velocity function entering the distal aorta inlet over time.....	17
Figure 2.7:	Isometric view of the mesh used for the fenestrated stent	20
Figure 4.1:	Model of the fluid fill of the healthy aortic bifurcation	24
Figure 4.2:	Model of the velocity contours within a healthy aortic bifurcation.....	24
Figure 4.3:	Model of the fluid fill of the unhealthy aortic bifurcation	25
Figure 4.4:	Model of the velocity contours of the unhealthy aortic bifurcation.....	26
Figure 4.5:	Model of the fluid fill of the kissing stent aortic bifurcation model.....	27
Figure 4.6:	Model of the velocity contours of the kissing stent aortic bifurcation model	27
Figure 4.7:	Model of the velocity vector map of the kissing stent aortic bifurcation model	28
Figure 4.8:	Model of the vorticity of the kissing stent aortic bifurcation model	28
Figure 4.9:	Model of the fluid fill of the ipsilateral main body stent aortic bifurcation model with a 5mm fenestration	29
Figure 4.10:	Model of the velocity contours of the ipsilateral main body stent aortic bifurcation model with a 5mm fenestration	30
Figure 4.11:	Model of the velocity vector map of the ipsilateral main body stent aortic bifurcation model with a 5mm fenestration	30
Figure 4.12:	Model of the vorticity of the ipsilateral main body stent aortic bifurcation model with a 5mm fenestration	31
Figure 4.13:	Model of the fluid fill of the ipsilateral main body stent aortic bifurcation model with a 10mm fenestration	32
Figure 4.14:	Model of the velocity contours of the ipsilateral main body stent aortic bifurcation model with a 10mm fenestration.....	32
Figure 4.15:	Model of the velocity vector map of the ipsilateral main body stent aortic bifurcation model with a 10mm fenestration.....	33

Figure 4.16: Model of the vorticity of the ipsilateral main body stent aortic bifurcation model with a 10mm fenestration.....	33
Figure 4.17: Model of the fluid fill of the ipsilateral main body stent aortic bifurcation model with a 15mm fenestration	34
Figure 4.18: Model of the velocity contours of the ipsilateral main body stent aortic bifurcation model with a 15mm fenestration.....	35
Figure 4.19: Model of the velocity vector map of the ipsilateral main body stent aortic bifurcation model with a 15mm fenestration.....	35
Figure 4.20: Model of the vorticity of the ipsilateral main body stent aortic bifurcation model with a 15mm fenestration.....	36
Figure 5.1: Zoomed in model of the velocity vectors of the kissing stent aortic bifurcation model.....	42
Figure 5.2: Zoomed in model of the velocity vectors of an early fenestrated stent design.....	43
Figure 5.3: Zoomed in model of the velocity vectors of the ipsilateral main body Stent aortic bifurcation model with a 10mm fenestration	45

List of Tables

Table 2.1:	Experimental parameters used throughout all fluidic simulations	20
Table 4.1:	Table of average mass flow rates for all simulations	36
Table 4.2:	Table of average velocities for all simulations	37

Acknowledgments

Special thanks to the following individuals for their advice, experience, opportunities, and support that lead to the development of this thesis:

- Dr. Mohamed Zayed
- Dr. Guy Genin
- Dillon Williams
- Sanghun 'Alex' Lee
- Dr. Eric Leuthardt
- Dr. Chao Yang
- Angelica V. Price

Special thanks to the following departments, groups, and/or organizations that helped contribute to this thesis work and opportunity:

- Washington University in St. Louis; Department of Engineering and Applied Science
- Washington University School of Medicine in St. Louis; Department of Surgery
- Washington University School of Medicine in St. Louis; Center for Innovation in Neuroscience and Technology
- Washington University in St. Louis; Dual-Degree Engineering Program

Special thanks goes to the Zayed Lab at Washington University School of Medicine in St. Louis, Department of Surgery, and the distinguished faculty within my department who have reviewed this thesis and helped support the related research.

Alexander J. Wirtz

Washington University in St. Louis

May 2018

Dedicated to my parents, Brad and Laurie Wirtz.
Thank you both for your continued and endless support of my education.

ABSTRACT OF THE THESIS

An Evaluation of Proposed and Current Cardiovascular Stent Design Approaches to Aortoiliac
Occlusive Disease

by

Alexander Joseph Wirtz

Master of Science in Mechanical Engineering

Washington University in St. Louis, 2018

Research Advisors: Professors Mohamed Zayed and Guy Genin

Aortoiliac occlusive disease is a subsequent disease of atherosclerosis involving the accumulation of plaque on the lining of the artery wall causing the artery lumen to narrow at the site of the aortic bifurcation. To prevent foreseeable embolization threats or ischemia, revascularization of the aortic bifurcation is commonly treated by arterial stenting. The most common practice of arterial stenting of aortoiliac occlusive disease is using balloon expandable stents. Traditionally, in order to prevent encroachment and/or occlusion of one iliac system by the stenting of the other, two balloon expandable stents are placed in the aortic bifurcation adjacently (kissing) at the time of deployment. The kissing stent procedure, while commonly used in clinical practices, has major disadvantages in the design. The stents used for this procedure are usually outside the Food and Drug Administration (FDA) approved Instructions For Use (IFU) and have suboptimal long-term patency. It is because of these real-world disadvantages that a novel aortoiliac, fenestrated (AIFEN), tapered, balloon expandable stent design has been proposed as a superior treatment technique to aortoiliac atherosclerotic occlusive disease. In this thesis, computer-aided design models of the aortic

birfucation have been generated and computation blood flow fluid dynamics were evaluated between the traditional kissing stent configuration and the novel AIFEN design. Additionally, three various length parameters involved with the design of the fenestration, at 5mm, 10mm, and 15mm, respectively, were simulated to provide an optimized alternative to the current solutions used in industry. Coefficients for comparative analysis including mass flow rate, average velocity at the common iliac outlets, velocity contours and vectors, and blood flow vorticity. Superiority of the AIFEN design treatment method over the kissing stent aortoiliac procedure, in addition to the best size fit of the fenestration needed for this procedure, is demonstrated in this thesis.

Chapter 1

Background

In this thesis background, the cardiovascular condition of aortoiliac occlusive disease will be reviewed, as well as currently used endovascular treatment techniques for the disease. A novel aortoiliac, fenestrated, tapered, balloon expandable stent design will also be proposed.

1.1 Aortoiliac Occlusive Disease

Aortoiliac occlusive disease, sometimes referred as Leriche syndrome, is a result of atherosclerotic plaque accumulation on the inner lining of the distal abdominal aorta and proximal common iliac arteries. Unimpeded blood flow in the aortoiliac segment is essential to provide pelvic arterial perfusion, and arterial inflow to the bilateral lower extremities. [1] Chronic progressive accumulation of atherosclerotic plaque in the distal aorta and common iliac arteries can cause a critical reduction in the blood flow to the lower extremities and pelvic organs such as the rectum, gonads, and perineum. [2] Critical obstruction or complete occlusion of the aortoiliac segment can lead to significant clinical morbidity lower extremity pain, ischemia, wounds/ulcerations, and risk of amputation. [3-4] It is important to identify patients who are at risk of progressive aortoiliac occlusive disease, and to provide them with durable treatment modalities that can restore luminal patency. A concept schematic of the aortic bifurcation with aortoiliac occlusive disease can be seen in Fig. 1.1.

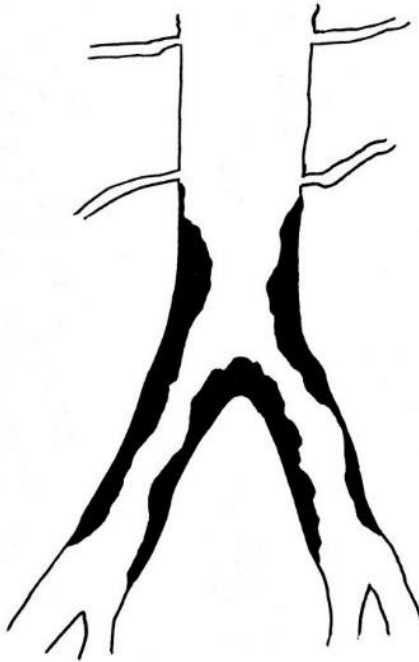


Figure 1.1 Schematic of the aortic bifurcation cross-section with aortoiliac occlusive disease. Plaque on the lining of the aortic bifurcation walls can be seen shaded in, narrowing the available lumen of the vessel.

Aortoiliac occlusive disease is thought to most arise from chronic turbulence at the aortic bifurcation. The encrustation hypothesis suggests that, with time, this turbulence leads to plaque accumulation on the walls of the artery. Individuals with risk factors such as advanced age, smoking, diabetes, hyperlipidemia, and/or hypertension are more likely to develop more progressive plaque accumulation in this bifurcation region as well as other arterial tree bifurcations such as the carotid arteries, renal arteries, and mesenteric arteries. [5-6] This does not limit individuals from the disease, however, as poor diet, poor exercise habits, and a family history of heart disease can increase the probability of accruing plaque as well. Approximately half of all patients with aortoiliac occlusive disease do not exhibit any symptoms before the more life-threatening symptoms appear, so accurate statistical evidence of the condition is unknown. However, with post-reports and diagnostics of aortoiliac occlusion disease, about 25% of the United States population over the age of 70 are estimated to be affected by this condition, with about 8.5 million people in the United States estimated to be affected overall. [6]

1.2 Current Treatment Solutions

To prevent foreseeable embolization threats or ischemia, revascularization of the aortic bifurcation is required in response to this disease. The most common practice resolving aortoiliac occlusive disease is endovascular surgery involving arterial stenting by balloon angioplasty. Balloon angioplasty is done by using catheter-based technology to pass a compressed stent through the cardiovascular system. [7] When a balloon catheter has been guided to the diseased vessel, the practitioner inflates the balloon, forcing the stent to decompress and expand to the diameter of the vessel. In this case, these stents are generally covered with a biocompatible plastic sheet that, with the metal stent as support, compresses and crush all of the plaque radially to the outer edge of the vessel. The balloon is then deflated and removed from the vessel, leaving a newly deployed stent in place. This restores blood flow through the diseased artery as the stent becomes plastically deformed to support the vessel indefinitely. [7]

It should be observed that stenting the aortic bifurcation is not as simple as stenting an ordinary vessel. Because the distal aorta forks into the two common iliac arteries, more complex solutions have been developed to stent the shape of the bifurcation. Solutions to this involve the use of bifurcation-shaped self-expanding stents. These stents, however, are recommended in arterial trees that are undergoing regular arterial deformation and where radial force is critical to maintain patency/stability of the artery. Because radial forces are needed to collapse the plaque on the outer walls of the bifurcation, balloon-expanding stent are generally used for this treatment procedure. In current practices, kissing arterial stenting with balloon angioplasty is used to treat aortoiliac occlusive disease. This procedure involves the use of two basic iliac stents being placed in the common iliac arteries, but also extending further into the distal aorta. The name is given to the practice due to both common iliac stent touching each other in the distal aorta. [8] However, this practice is not currently approved by the FDA, but produces the best outcome in restoring patency to the aortic bifurcation. All current FDA-approved aortic stents on the market are self-expanding and are intended for the treatment of aneurysmal disease rather than atherosclerotic aortoiliac occlusive disease, thus there is a lack of clinically ready technology in this area. A schematic of the kissing arterial stenting practice can be seen in Fig. 1.2.

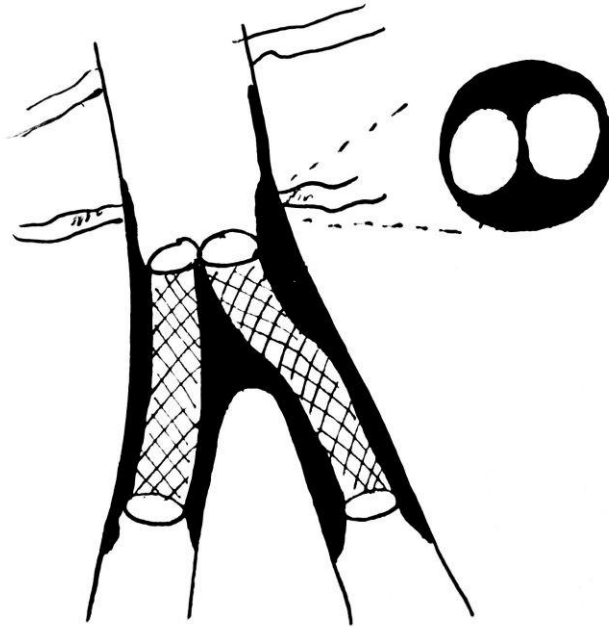


Figure 1.2 Schematic of the aortic bifurcation with placed kissing stents and observable cross-section. Compressed plaque has been shaded and the cross-section provided, located in the distal aorta, represents the inlet of the kissing stent procedure.

A significant portion, if not all, discrepancies from the kissing stent procedure are consequence from the inlet of the two stents in the distal aorta. A short answer to this issue is simply that these two iliac stents are designed to only exist in the common iliac arteries; the stents are not intended to be interacting with each other or be placed in the distal aorta. In clinical practice, a large amount of variability occurs at the inlet of these kissing stents. When setting these stents in a patient, a practitioner will arrange the stents in a fashion that will least likely harm the patient. This can be seen by two different cross-section situations, for example, in images A and B in Fig. 1.3. Cross-section A in Fig. 1.3 represents a situation where arterial pressure is an issue. Because the practitioner does not want to rupture the distal aorta when deploying these stent, the stents will not be fully decompressed and expanded to the inner diameter of the distal aorta. Therefore, two smaller stent opening will divert blood flow to the two common iliac arteries. This introduced several issues. First, because the stents have not decompressed to fill the maximum diameter of the vessel they exist in, the amount of blood flow that travels to the lower extremities is inhibited. Consequentially, blood will flow pass and around these stent into various gaps in the plaque as the area surrounding the two kissing stent inlets is not entirely solid. This will cause immediate thrombosis, or blood

clotting, that can put a patient at life-threatening conditions due to an embolism, or traveling blood clot, in their cardiovascular system. Another significant issue is the offset of the two stents such that the alignment of the stents is not symmetrical with the rest of the body. Because the combination of these two stents will, more than likely, not create a symmetric inlet, an increase in fluid flux will occur in the stents. This will cause the vorticity to increase due to blood spiraling through each iliac stent to reach the iliac arteries. This is problematic due to potential of stagnation, mixing, and turbulent flow that can cause thrombosis to occur.

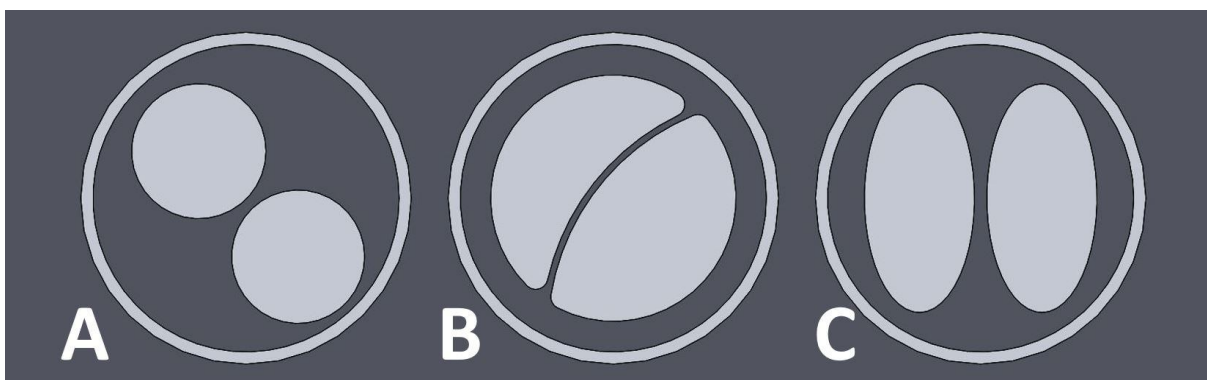


Figure 1.3 Schematic of the various cross-section found at the inlet of the kissing stents procedure. The cross-sections exist in the distal aorta and are CAD renditions of expected results based on literature. (A) cross-section showing kissing stents protocol when arterial integrity is at risk. (B) cross-section showing typical kissing stent cross-section when stents are fully decompressed. (C) ideal kissing stents cross-section used for the analysis in this thesis to establish the inferiority of the ideal situation to the AIFEN design.

Looking at cross-section B in Fig. 1.3, the stents appear to be fully decompressed. However, the pressure from each stent actually causes one to concave and the other to convex, as shown. This is commonly what happens in practice due to the forces stents exert in blood vessel. This introduces more significant issues in the design of the inlet. First, the amount of residual stress present at this inlet is very hazardous for the patient. A potential rupture of the distal aorta is likely to occur as the stents are not designed to interact with one another. This large presence of stress can also cause kinks in the stents to occur, causing a complete blockage of blood flow to lower extremities. [10] Additionally, a similar issue of vorticity that was introduced in cross-section A will occur in cross-section B. Because the stents are asymmetrical at the inlet, and more so than image A due to a non-circular cross-section per stent, a large vorticity would be expected in these stents causing potential thrombosis. [28] Essentially, placing stents in this aortic bifurcation that causes conditions to appear

that would not originally be present in a healthy aortic bifurcation is a clear sign for flaws in design. Image C in Fig. 1.3 better represents what was seen in the schematic in Fig. 1.2 and what will be assumed for this thesis to show that the most ideal situation of the kissing stent procedure is still inferior to the proposed AIFEN stenting procedure. A CT scan image of kissing stents in the distal aorta can be seen in Fig. 1.4.

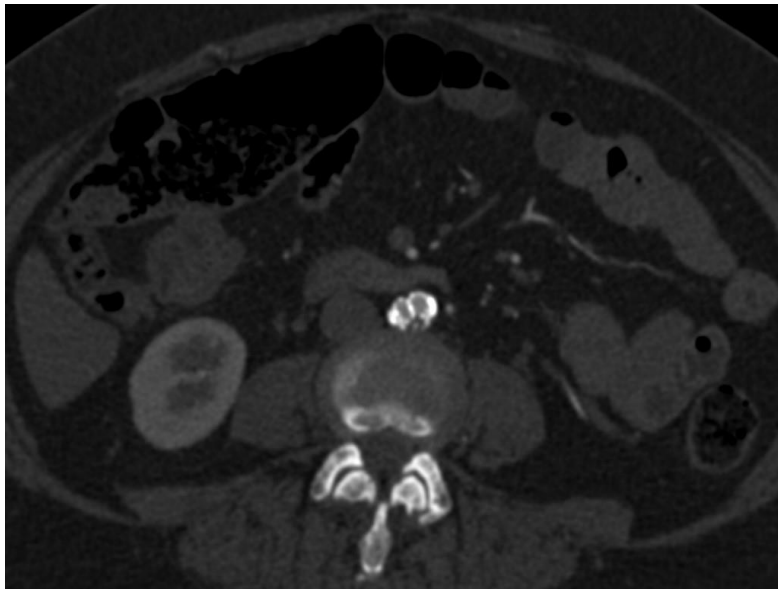


Figure 1.4 CT scan showing the presence of kissing stents in the distal aorta.

For more serious cases or if minimally invasive balloon angioplasty is not suitable for the patient, open surgery is the next option to treat vascular disease. Open surgery would require an aorto-bi-femoral or an aorto-bi-iliac bypass graft to be placed. This involves the rerouting of blood flow around the diseased vessel while a self-expanding graft is surgically placed. The graft is all in one piece and is more form fitted to the shape of the aortic bifurcation. [9] This is, however, a fairly morbid surgical procedure that can have a long recovery time. Additionally, most patients cannot tolerate such an invasive procedure that involves large revascularization due to concomitant coronary artery disease, cerebrovascular disease, or advanced age. Alternatively, endovascular treatment modalities with angioplasty and, because of this, stenting has become more prevalent over the past two decades. This is supported by several clinical trials that have demonstrated angioplasty of the iliac arteries alone is not durable and has low long-term patency results. [29] Since then, studies have shown that stenting of the iliac arteries is much more durable, and particularly balloon

expandable stents in the common iliac arteries have found to be quite robust. [29] Because of these results, the analysis found in this thesis will only consist of arterial stenting techniques done by balloon angioplasty in favor of minimally invasive techniques.

1.3 Discussion of Proposed Design

The kissing arterial stenting procedure, while commonly used in practice, has major disadvantages in design. The method itself is not FDA approved, and is an adaptation of the best use of balloon-expandable stents to treat aortoiliac occlusive disease currently with many notable issue involved with the inlet design of the procedure. It is because of these numerous concerns and design issues that this novel fenestrated stent is introduced.

1.3.1 Device Introduction

This novel fenestrated stent design is constructed to overcome the major disadvantages involved in treating aortoiliac occlusive disease. Ultimately, this design is a balloon expandable tapered stent designed to treat the aortic bifurcation that includes a fenestration to allow antegrade blood flow to the contralateral common iliac artery immediately after deployment. The proposed stent is designed to act as a single, ordinary stent in the aortic bifurcation with a fenestration that will remove the need to perform a bypass on the patient during the angioplasty procedure due to immediate antegrade blood flow to the contralateral common iliac artery. This unique, fenestrated stent will be referred to as the ipsilateral main body aortoiliac stent. Additionally, a secondary, contralateral complementary iliac stent can be placed in the contralateral common iliac artery in tandem with the ipsilateral main body stent in order to treat the occlusive disease for the entire bifurcation. This complementary stent will be placed into the fenestration and flared out by balloon angioplasty techniques to establish a smooth, transitional path for blood flow in the entire bifurcation. This flared technique is technology that has already been established and is being used in the industry, such as in the stenting the renal arteries. [30] Complementary to that, fenestrated stents are also established and used in industry as well due to their corresponding use with the flared technique. [31] Currently, the market for medical devices in vascular surgery treatment of aortoiliac occlusive

disease does not support nearly any balloon expandable stents, especially stents of this novelty. This is because most stents, even those using fenestration and flared stenting techniques, used in treating occlusive disease are self-expanding and are intended/ designed for aneurysmal disease treatment. Thus, a need for this new technology in industry is very prevalent. A schematic of this prototype design concept can be seen in Fig. 1.5.

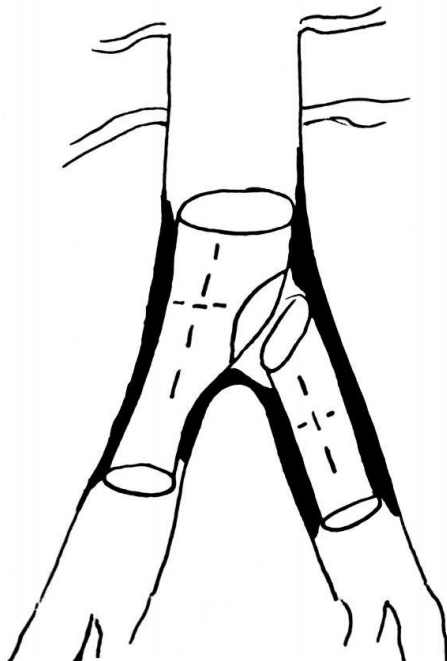


Figure 1.5 Schematic of the aortic bifurcation with the ipsilateral main body aortoiliac stent design in place. Additionally, a contralateral complementary iliac stent has been placed to demonstrate the entire treatment of the aortic bifurcation. It should be noted that the complementary stent will be flared to the ipsilateral main body stent, contrary to the positioning in this schematic.

1.3.2 Model and Description of Device

This unique, fenestrated, ipsilateral main body aortoiliac stent will be placed in the distal aorta and one common iliac per the typical method of balloon angioplasty. Once the stent is positioned in the diseased vessel, a series of specifically placed radiopaque markers on the catheter will allow the practitioner to arrange the stent such that the fenestration is facing the contralateral common iliac. [11] The balloon will then expand to allow the stent to form to the inner walls of the vessel and crush the plaque to create a new lumen for blood flow and thus restoring patency. Due to the tapered design, the stent will fit more securely with the shape of the aortic bifurcation and will not

produce any more residual stress than necessary to create a new lumen in the vessel. A tapered stent is rarely seen in industry for occlusive disease treatment of this type, making this device novel. The fenestration itself will be secured with a metal wire for support in later flaring methods. Due the oval-shaped fenestration in position with the contralateral common iliac artery, antegrade blood flow can immediately resume to the lower extremities on both sides of the patient and thus removing any need for an invasive blood bypass. A primary feature of this fenestration is to treat aortoiliac occlusive disease where, in contrary, most other stents used for the aortic bifurcation are used to treat aneurysms. At this point, a second, similar procedure can be done to place the contralateral complementary stent in the contralateral iliac artery to completely treat the aortic bifurcation for occlusive disease. This is done by extending a small portion of the complementary iliac stent into the fenestration of the ipsilateral main body stent and flaring the stent via an angioplasty balloon. A schematic and feature breakdown of the device can be seen in Fig. 1.6.

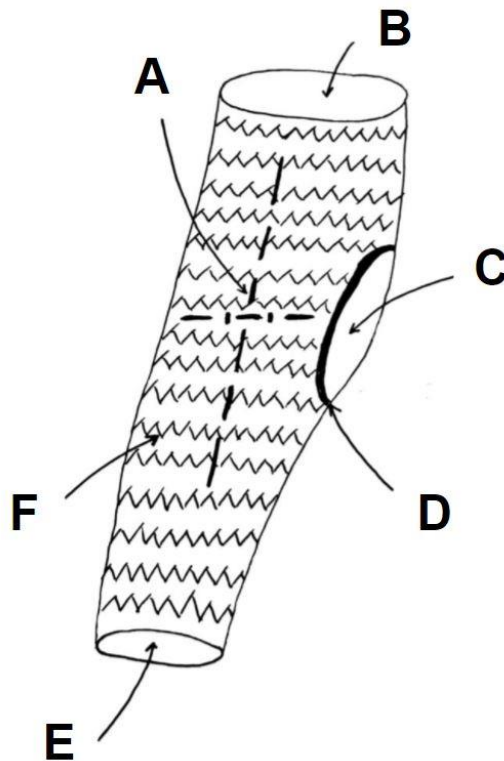


Figure 1.6 Schematic of the fenestrated stent design with labeled features. These features include: (A) radiopaque positional markers, (B) distal aorta end of the stent, (C) oval-shaped fenestration for optimal blood flow to contralateral common iliac, (D) radiopaque wireframe on fenestration border, (E) common iliac end of the stent that has been tapered down from aorta side, and (F) stent wireframe mesh over plastic cover.

1.4 Overview of Thesis

The purpose of this thesis is to introduce this novel AIFEN stent as a superior solution to the kissing arterial stenting angioplasty currently used in cardiovascular surgery practices. To justify the superiority of the stent over current practices, a simple computational fluid dynamic (CFD) simulation of both procedures has been conducted in order to determine if the proposed stent shares relatively equal performance in managing blood flow. Additionally, stagnation will be observed in order to determine if blood clotting in the aortic bifurcation occurs due to the introduction of these two stenting procedures. Because minimally invasive surgery is desired for this treatment, the aorto-iliac bypass or any other bypass-related solution will not be considered in this analysis. Six models will be analyzed in total: a healthy aortic bifurcation, an unhealthy aortic bifurcation, the kissing stents procedural treatment, and three proposed AIFEN stent treatment designs. These three AIFEN design will each include a different length parameter for the fenestration of 5mm, 10mm, and 15mm, respectively, in order to observe the various effects of altering the size of this fenestration in order to optimize the design as a whole. A limited number of fenestrations will be observed primarily because the design of the fenestrated stent is in its initial prototyping phase and is undergoing this preliminary analysis to establish advancement of the device over current practices. An image of the prototype concept for the ipsilateral main body aortoiliac stent can be seen in Fig. 1.7.



Figure 1.7 Initial prototype concept for the fenestrated stent.

Chapter 2

Methods

All experimental methods of this thesis are accomplished and analyzed with computer-aided design and computation fluid dynamics software. In this thesis methods, a careful breakdown of experimental models, fluid dynamic theory, and parametric studies are described in detail.

2.1 Models for the Aortic Bifurcation

In order to observe and develop simulations for the aortic bifurcation, six models were created using computer-aided design (CAD). CAD models of a healthy and an unhealthy aortic bifurcation were developed to compare the performance of each stenting procedure to a normal and worst-case situation. The healthy bifurcation was developed with a distal aorta inner diameter of 22mm and a common iliac diameter of 12mm. The bifurcation was created symmetrically with an angle of 25 degrees from the vertical. The length of the distal aorta present in the healthy model is 40mm and the length of both common iliac arteries present is 30mm. The unhealthy bifurcation was developed with a distal aorta inner diameter of 12mm and a common iliac diameter of 6mm. This was created with the assumption that aortoiliac occlusive disease can commonly occlude the vessels up to 50% in diameter reduction when significant symptoms start to appear. [12] The bifurcation, similarly, was created symmetrically with an angle of 25 degrees from the vertical. The length of the distal aorta present in the unhealthy model is 40mm and the length of both common iliac arteries present is 30mm. [13] The cross-sections of these two CAD models can be seen in Fig. 2.1.

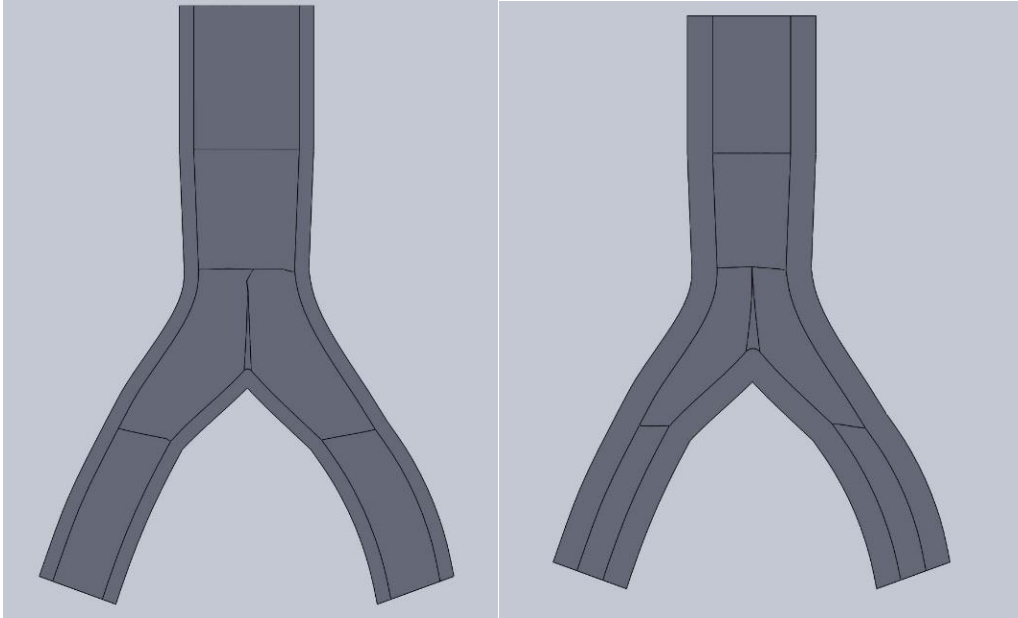


Figure 2.1 Image of the CAD cross-sections of the healthy aortic bifurcation model (left) and the unhealthy aortic bifurcation model (right). Note dimensions in the text for accurate modeling of the aortic bifurcation.

The kissing stent procedural CAD model was created using similar techniques to that of the previous two bifurcations. Because an expected 10-20% stenosis of the vessels is present once the stents expand, an aortic inner diameter of 20mm and common iliac inner diameter of 9mm were used for this model. [14] The kissing stents were created with an ideal spline that would match the probable way the stent would expand in the vessels. These stents are fractions of a millimeter thick, so there are small lips present in the model at the inlets and outlets of these stents. The inlet of blood flow from the distal aorta to the kissing stents is modeled as a flat face into two oval-opening stents, similar to image C in Fig. 1.3. These kissing stents are held at a constant inner diameter throughout the stented portion of the model, with the exclusion of the inlet. The cross-section of this CAD model can be seen in Fig. 2.2 and a wireframe image of the entire model can be seen in Fig. 2.3 for clarity purposes.

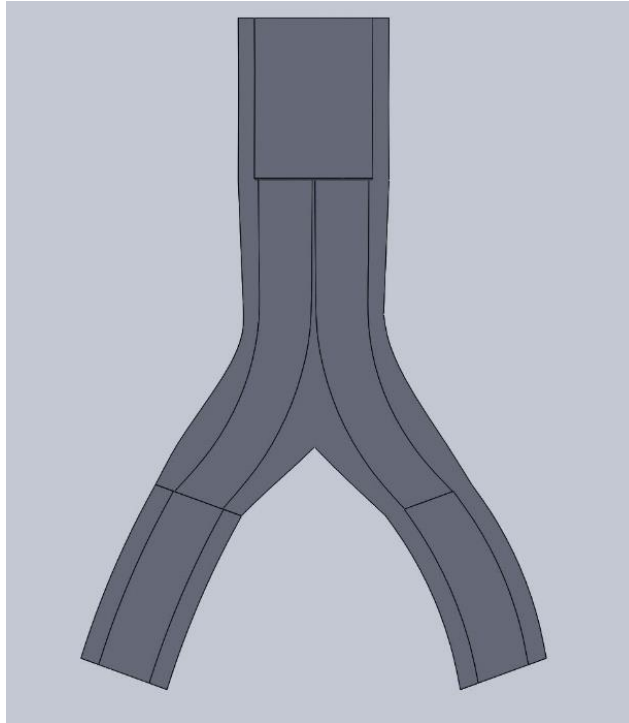


Figure 2.2 Image of CAD cross-section of the aortic bifurcation model with placed kissing stents.

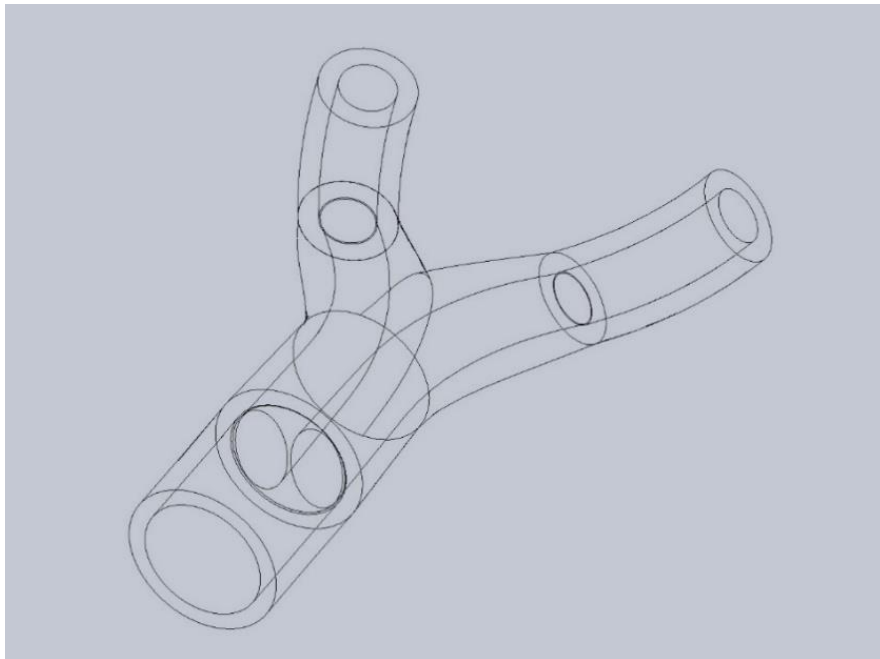


Figure 2.3 Image of CAD wireframe view of the aortic bifurcation model with placed kissing stents.

To optimized and discover the proper size of the fenestration in the ipsilateral main body stent, three CAD models of the fenestrated stent were created. The three models only differ in size of the fenestration with diameter lengths of 5mm, 10mm, and 15mm for the models, respectively. The novel fenestrated stent CAD models were created using similar techniques to that of the previous bifurcations. Similar to the kissing stent aortic bifurcation model, an expected 10-20% stenosis of the vessels is present once the stents expand. Thus, an aortic inner diameter of 20mm and common iliac inner diameter of 9mm were used for all three models. Unlike the kissing stents, the stents used in this model were not held at a constant inner diameter due to the tapered intent of the device. The fenestrated stent was created with a proper spline that would match the ideal way the stent would expand in the vessel, and the fenestrated was cut out in an oval fashion. The length noting the difference in these models refers to the longer diameter of the oval, lengthwise, which is viewable in Fig. 2.4. These stents are fractions of a millimeter thick, so there are small lips present in the model at the inlets and outlets of these stents. The complementary contralateral iliac stent is placed in the contralateral common iliac in an expected flared fashion with the fenestration for complete treatment of the aortic bifurcation. The complementary iliac stent was tapered from the flared fenestration to match the expected sizing of the contralateral common iliac artery. The cross-sections of these CAD models can be seen in Fig. 2.4 and a wireframe image of the entire model, 10mm fenestration only, can be seen in Fig. 2.5 for clarity.

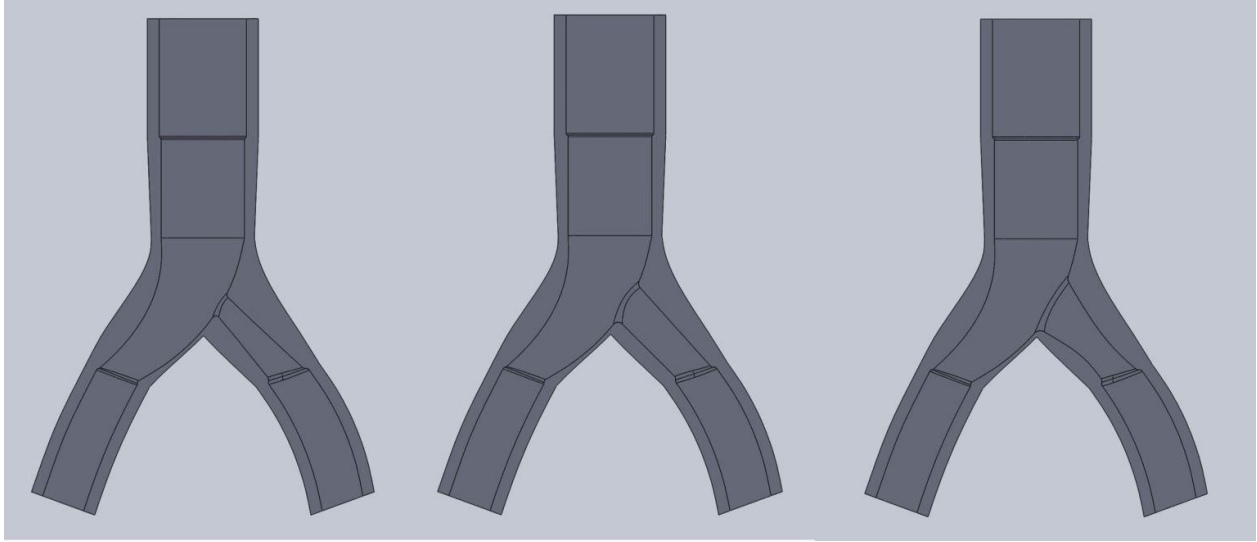


Figure 2.4 Image of CAD cross-sections of the aortic bifurcation models with the fenestrated stent designs. The fenestrations vary, causing the complementary stent to taper to the size of the common iliac in certain cases. The fenestration sizes are 5mm (left), 10mm (middle), and 15mm (right) for the three models.

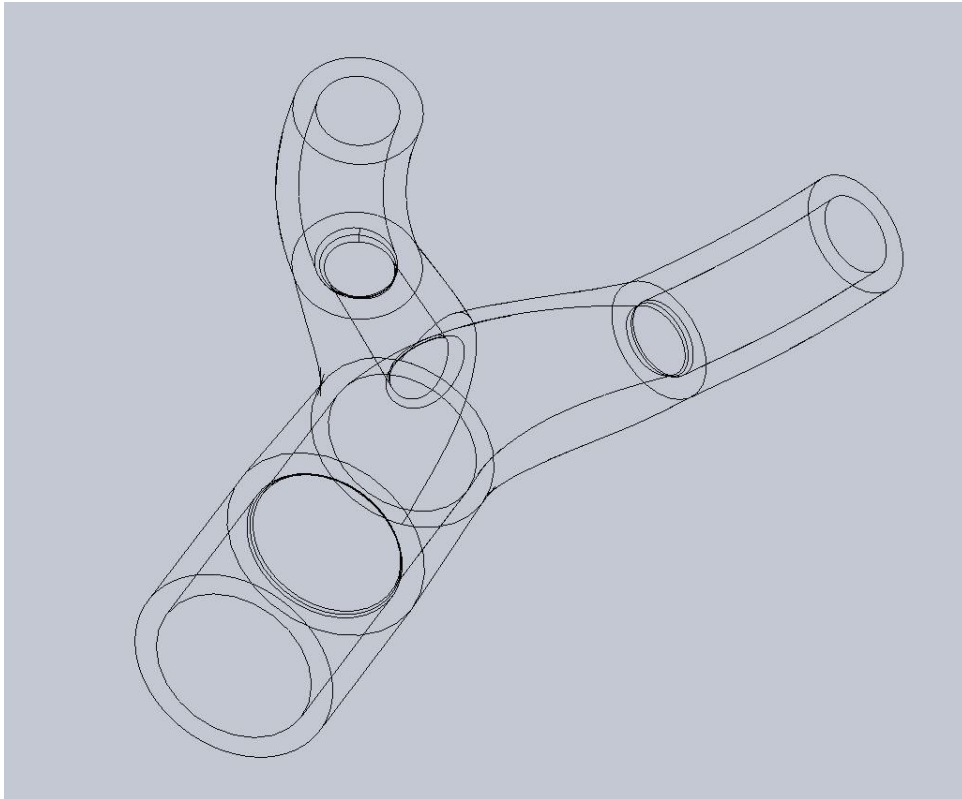


Figure 2.5 Image of CAD wireframe view of the aortic bifurcation model with the proposed AIFEN stent design. This model includes a 10mm fenestration in the ipsilateral main body aortoiliac stent.

2.2 Boundary Conditions and Assumptions

A few assumptions were made for CFD analysis of these four models. First, the stent and arterial walls of the model are set to be rigid. [15] This is because a goal of this thesis is to determine the ability of the fenestrated stent to redirect blood optimally in comparison to the kissing stent procedure. Because there is more significance in the outcome of the fluid dynamics, the forces and shear placed on the vessel walls are neglected. This will be observed in later optimization phases. Additionally, the inner walls of the stent and artery are modeled to be smooth. The stent itself is modeled such that the wire mesh is on the outside of the plastic PTFE covering.

Boundary conditions were set for the inlet of the distal aorta, the outlets of the common iliac arteries, and the inner walls of the model. For the arterial wall and inner stent wall, the velocity is set to zero. For each of the common iliac artery outlets, a pressure of 100 mmHg was used. [16] For the inlet, a written inlet velocity function was used to simulate the phenomenon of blood pumping into the distal aorta. [17] The scaling of this velocity plot was adjusted due to similar functions and results found in the literature. [18] A representation of this function can be seen by the following Fourier series:

$$v_{blood,inlet} = C_0 \left(\sum_{n=0}^8 a_n \cos(n\omega t) + b_n \sin(n\omega t) \right) \quad (2.1)$$

A plot of this blood velocity over time can be seen in Fig. 2.6. This function can be seen in detail in the appendix of this thesis with the appropriate constants C , a , ω , and b .

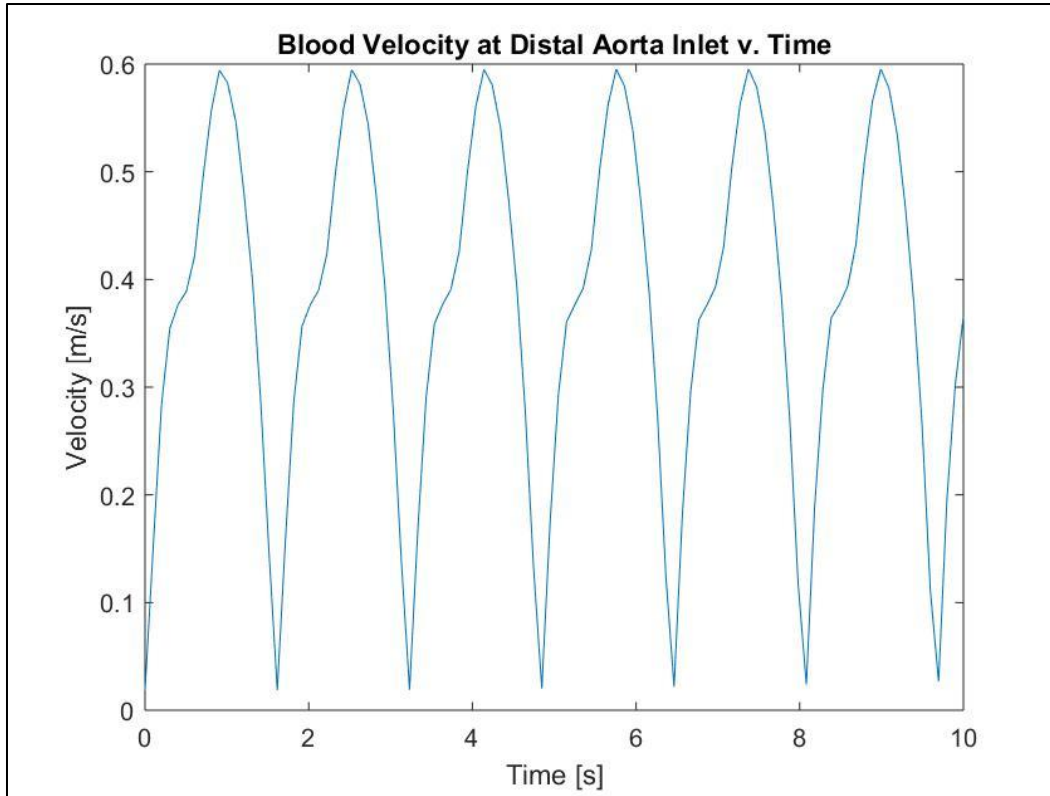


Figure 2.6 Plot of the blood velocity function entering the distal aorta inlet over time.

2.3 Discretization

Due to the assumptions made for this simulation, this stent fluid problem can be approached like any other common fluids problem. The governing equations for this simulation uses some of the most fundamental equations in fluid dynamics: the Navier-Stokes equations and the continuity equation. The continuity equation is as follows:

$$\frac{\partial \rho}{\partial t} + \nabla \cdot (\rho \vec{v}) = 0 \quad (2.2)$$

such that ρ is density, t is time, and v is velocity. [19] However, because blood is observed as an incompressible fluid and thus density does not change as a function of time, the above equation can be simplified to:

$$\nabla \cdot \vec{v} = 0 \quad (2.3)$$

The common form of the Navier-Stokes equation is as follows:

$$\rho \left(\frac{d\vec{v}}{dt} + \vec{v} \cdot \nabla \vec{v} \right) = -\nabla p + \mu \nabla^2 \vec{v} + \rho \vec{g} \quad (2.4)$$

such that p is pressure, g is gravity, and μ is the dynamics viscosity coefficient. [19] It is important to note the significant issue with viscosity in this equation as blood is a non-Newtonian fluid. To simulate this in the fluid dynamics software, the Carreau fluids model will be used to model the variable behavior of viscosity as a function of shear rate. This can mathematically be shown as follows:

$$\mu_{eff}(\dot{\gamma}) = \mu_{\infty} + (\mu_0 - \mu_{\infty}) (1 + (\lambda \dot{\gamma})^2)^{\frac{n-1}{2}} \quad (2.5)$$

where μ_{eff} is the effective viscosity, μ_{∞} is the infinite-shear viscosity, μ_0 is the zero-shear viscosity, n is the power-law index, λ is the time constant, and $\dot{\gamma}$ is the shear rate. [6] With this model built in the software, the simulation can better represent blood flowing through the vessels and stents using the fundamental equations described in Eq. 2.3 and Eq. 2.4.

2.4 Software

2.4.1 Solidworks

In order to create fluid models for this thesis, SolidWorks CAD software was used (Dassault Systèmes, Vélizy-Villacoublay, France). This software utilizes a parametric feature-based approach to create 3D modeled parts. Additionally, full assemblies of parts and drawings can be created using SolidWorks. The software has a series of add-on applications of computer-aided engineering (CAE) that allow the user to perform various analyses on the parts or assemblies, such as finite element

analysis. For this thesis, six models of the aortic bifurcation were created based on the literature and imported into ANSYS Fluent for fluid dynamics calculations. [20]

2.4.2 ANSYS Fluent

In order to analyze and determine fluidic properties from the CAD models of the aortic bifurcation, ANSYS Fluent was utilized (ANSYS, Canonsburg, Pennsylvania, USA). Fluent is capable of modeling fluid flow, heat transfer, turbulence, and pressure gradients in a single simulation. Users can select either external or internal flow models, set boundary conditions and material properties, and model/plot outcomes of desired simulations involving numerous fluid characteristics. For this thesis, the six CAD models were imported, internal flow was selected, boundary conditions were selected, properties of blood, artery, and PTFE were used, a mesh was created, desired flow properties were selected, and data was collected over a specified time step. [21] Simulations were ran multiple times to establish minimal variability across each simulation and remove the possibility of any internal error.

2.5 Experimental Parameters

The listed parameters in Table 2.1 were used for all experimental simulations described in this thesis, which includes all parameters used for the Carreau-model. The CFD simulation in ANSYS Fluent was prepared using a pressure-based, absolute velocity solver in transient-state time. The experimental scheme was set to the default simple analysis structure and the spatial discretization used included a least squares cell based gradient, second order pressure differential, and second order upwind momentum where the transient formulation was set to first order implicit. Additionally, default under-relaxation factors were used and the preprogramed hybrid initialization method was selected. [22] A sample image of the mesh used for the fenestrated stent can be seen in Fig. 2.7.

Table 2.1 Experiment parameters used throughout all fluidic simulations. [22-23]

<i>Blood Density, ρ_{blood}</i>	1060 kg/m^3
<i>Artery Density, ρ_{artery}</i>	1160 kg/m^3
<i>Inner Stent, PTFE Density, ρ_{PTFE}</i>	2200 kg/m^3
<i>Outlet Pressure, p_{out}</i>	100 mmHg
<i>Time Constant, λ</i>	3.313 s
<i>Power – Law Index, n</i>	0.3568
<i>Zero Shear Viscosity, μ_0</i>	0.056 $kg/m \cdot s$
<i>Infinite Shear Viscosity, μ_∞</i>	0.0035 $kg/m \cdot s$
<i>Mesh Size</i>	200,000 – 500,000 <i>elements</i>
<i>Time Step</i>	0.1 s
<i>Time Span</i>	20 s

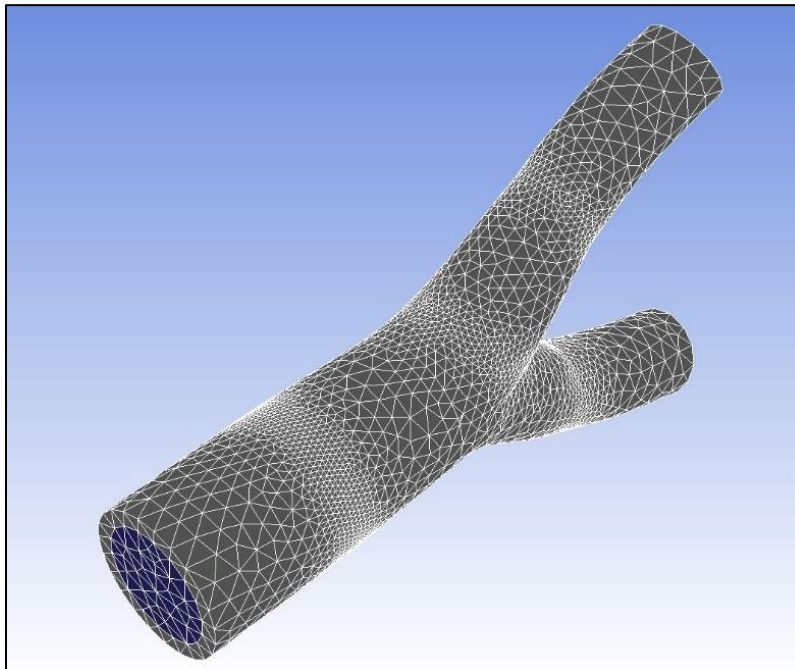


Figure 2.7 Isometric view of the mesh used for the fenestrated stent.

2.6 Parametric Studies

The primary goals of the thesis are to assess the potential of the fenestrated stent angioplasty procedure relative to the current standard of treatment for aortoiliac occlusive disease. In order to accomplish this, data has been obtained for each of the six aortic bifurcation models discussed in section 2.1. This includes determining average velocity at inlets and outlets, plotting velocity and vorticity, and evaluating points of stagnation via velocity vectors. Ultimately, the design of the fenestrated stent aims to minimize vorticity, achieve no stagnation, evenly distribute outlet mass flow rates, normalize outlet velocities, minimize pressure concentrations, and developed ideal streamline conditions. A brief optimization experiment will be conducted in comparing the results from the three various fenestration designs for the AIFEN stent models. All of these conditions and parameters will be evaluated across the six models in order to determine the performance, optimization, and progress that the fenestrated stent has made in being introduced into vascular surgery applications.

Chapter 3

Convergence Studies

In this thesis study, performance was observed in terms of basic principles of mass flow rate, outlet velocity, and high concentrations of vorticity. The study of fluid dynamics through vascular stents is something that has been observed over numerous years. Various analysis on stenting blood vessel includes observing the performance of various stent meshes, the stress induced on the vessel walls due to the stents, and the effects of vascular deformation due to stenting.

Similar studies in the literature discuss location of high flow disturbance occurring at the end of the stent and near the bifurcation arch itself. Similar results were found in this thesis study and will be taken into account. [24]

Additionally, it was observed in the literature that shear stress and stresses due to inflation of the stent have significant effects on the vasculature. It will be noted in future studies to perform similar tests to that of this thesis with deformable walls in the CFD analysis. [25]

Furthermore, studies on the performance of kissing stents in patient have been observed as well. Kissing stent patency has been shown to be very good in initial years, but degrade over time. [26] However, it is still praised as the best solution to aortoiliac occlusive disease as no other solutions have a presence in medical practice today. In terms of fenestrated stents, most analysis has been done on bridging stents grafts, which, while similar, are more primarily used in aneurysm and focus on treating other diseases other than occlusive disease. [27]

Overall, because this study is focused on the performance of a new alternative to the kissing arterial stenting procedure, the analysis produced will be novel in determining performance of a balloon-expandable fenestrated stent that treats aortoiliac occlusive disease.

Chapter 4

Results

CFD simulations were performed in the ANSYS Fluent environment to assess the performance of the kissing and fenestrated arterial stenting procedures. Flow fields at a healthy and an unhealthy bifurcation were first estimated as a comparison case.

4.1 Healthy Bifurcation

Fig. 4.1 displays the inner fill used to simulate the healthy aortic bifurcation. The healthy aortic bifurcation model was used in order to create a fundamental understanding of the best-case scenario of results that the flow would produce. The velocity contour map (Fig. 4.2) of the healthy aortic bifurcation showed the expected symmetric velocity field. The peak velocity magnitudes over the course of a cycle occurred near the exits and reached a maximum of 1.33 meters per second. Over the course of cardiac cycle, the vorticity showed a peak value near the exits of 2930 radians per second. Finally, the streamlines in the healthy aortic bifurcation, which represent the magnitude and directionality of the dimensional velocity field, largely followed the inner contours of the aorta.

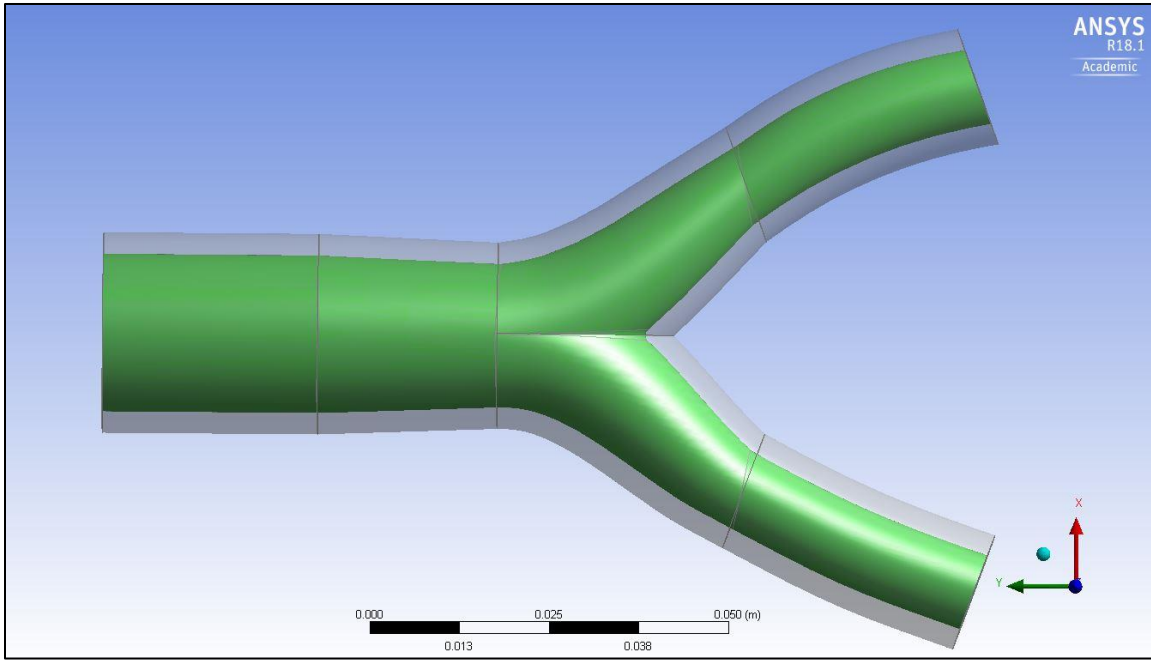


Figure 4.1 Model of the fluid fill of the healthy aortic bifurcation.

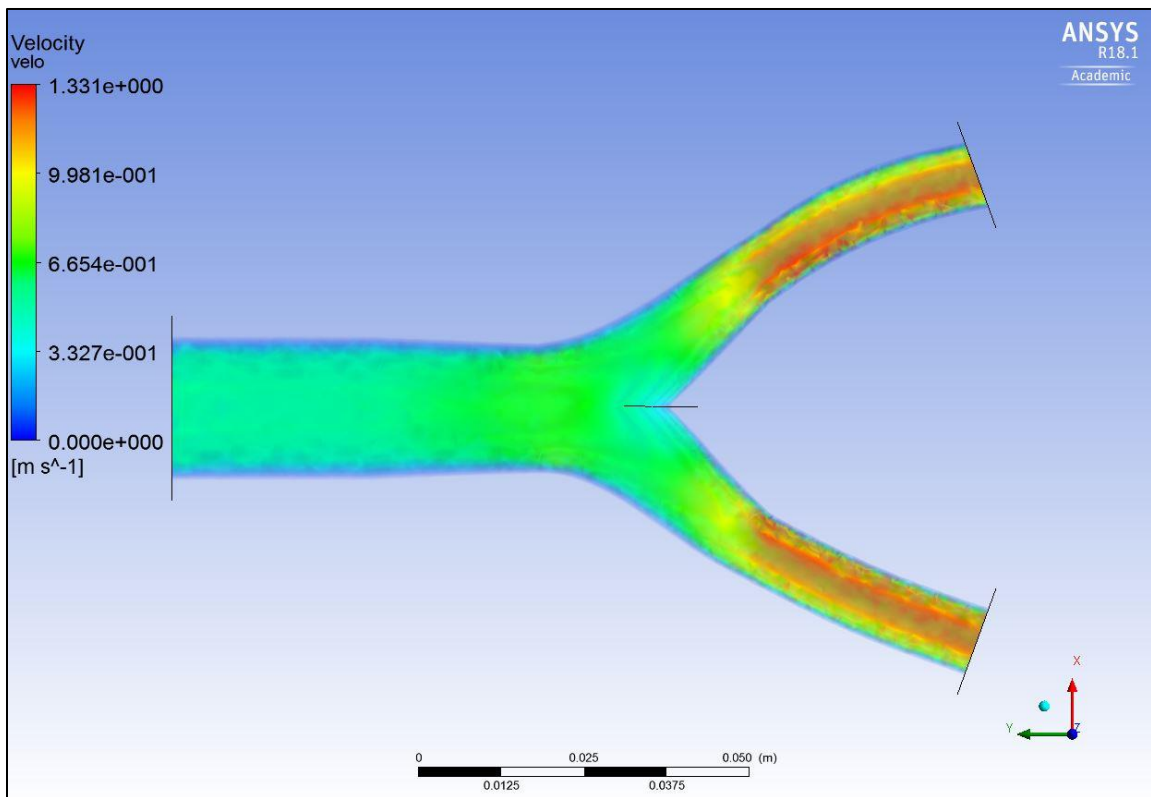


Figure 4.2 Model of the velocity contours within a healthy aortic bifurcation.

4.2 Unhealthy Bifurcation

The flow fields in the idealized unhealthy aortic bifurcation (Fig. 4.3) were studied as a worst-case comparison situation. Velocity (Fig. 4.4) fields were qualitatively similar to those of the healthy bifurcation, as were the streamlines. However, the magnitudes were different as to be expected. The peak velocity through the constricted aorta increased to 2.78 meters per second, and the peak vorticity increased to 12200 radians per second.

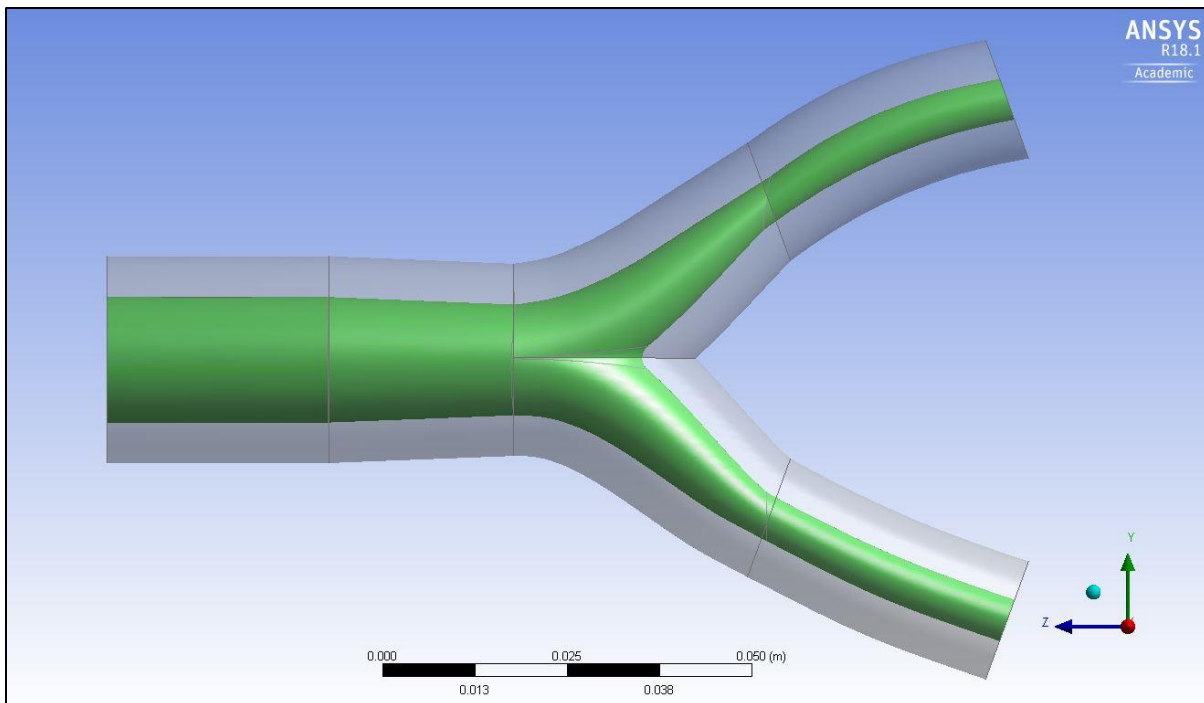


Figure 4.3 Model of the fluid fill of the unhealthy aortic bifurcation.

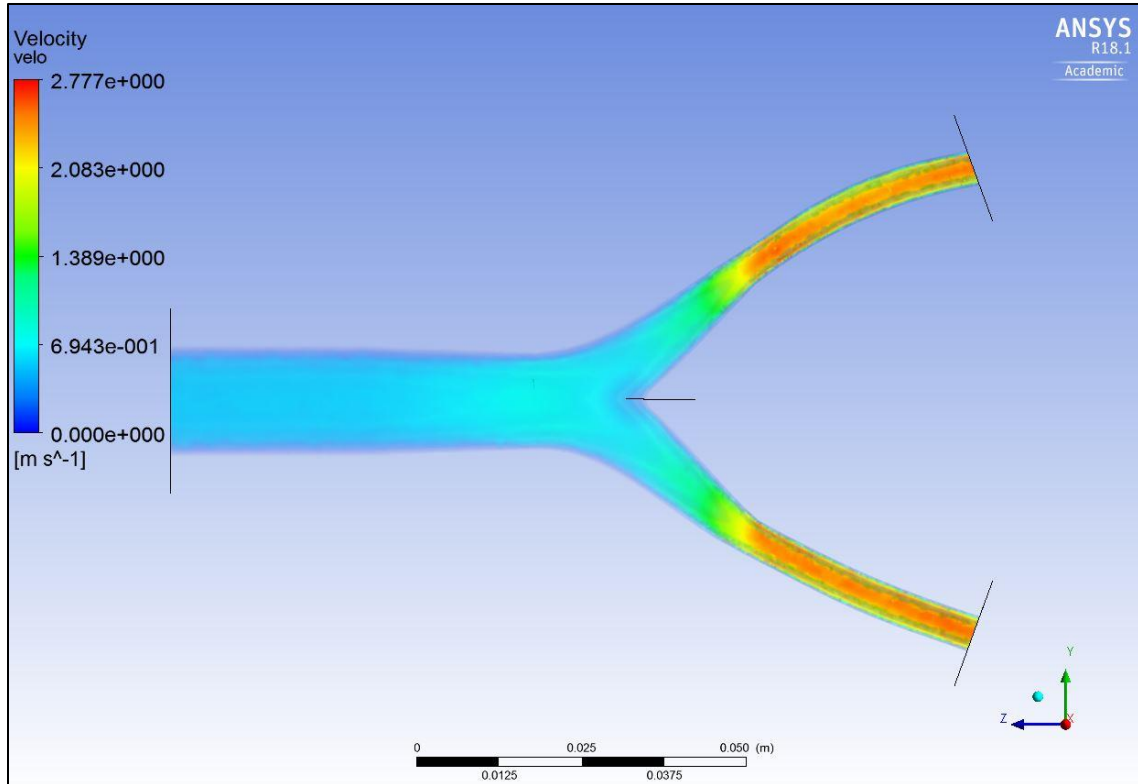


Figure 4.4 Model of the velocity contours of an unhealthy aortic bifurcation.

4.3 Kissing Stents

The kissing arterial stenting angioplasty procedure (Fig. 4.5) altered the flow fields from the two baseline cases. Velocity contours (Fig. 4.6) showed a sharp acceleration at the stent bifurcation and a peak velocity of 1.86 meters per second was recorded. Superimposing the image of the stent with the vector field (Fig. 4.7) revealed a change of flow direction occurring near the inlet of the two kissing stents in the distal aorta. Vorticity fields (Fig. 4.8) showed a maximum vorticity occurring near the inlet of two kissing stent. Streamlines largely followed the stent contours.

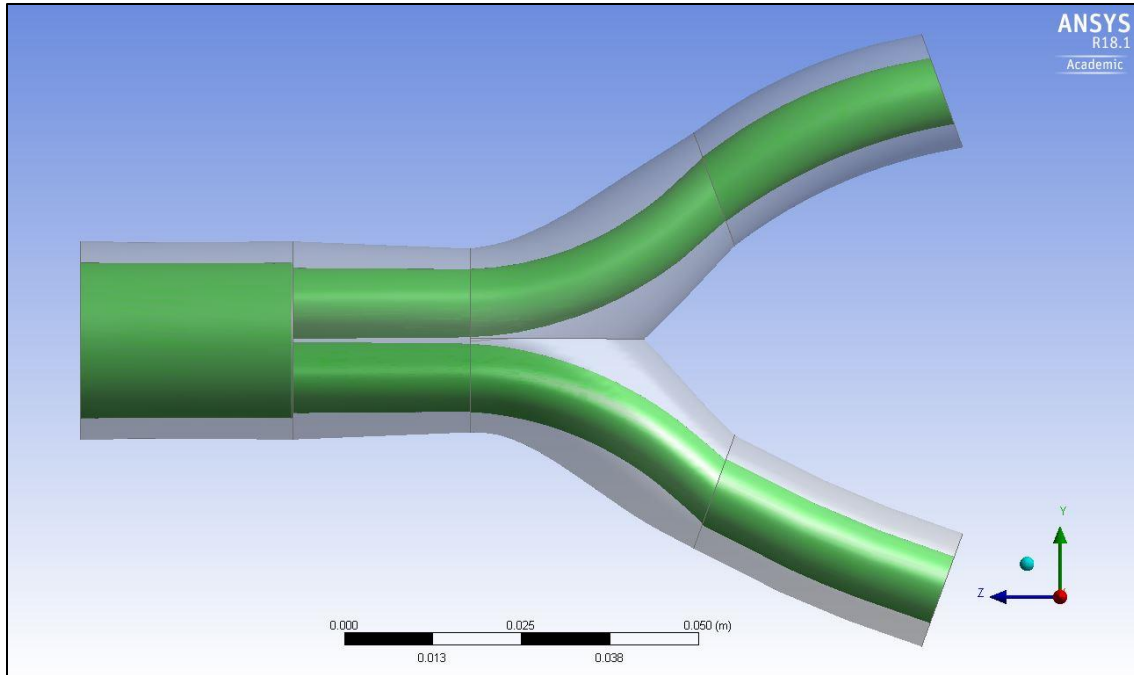


Figure 4.5 Model of the fluid fill of the kissing stent aortic bifurcation model.

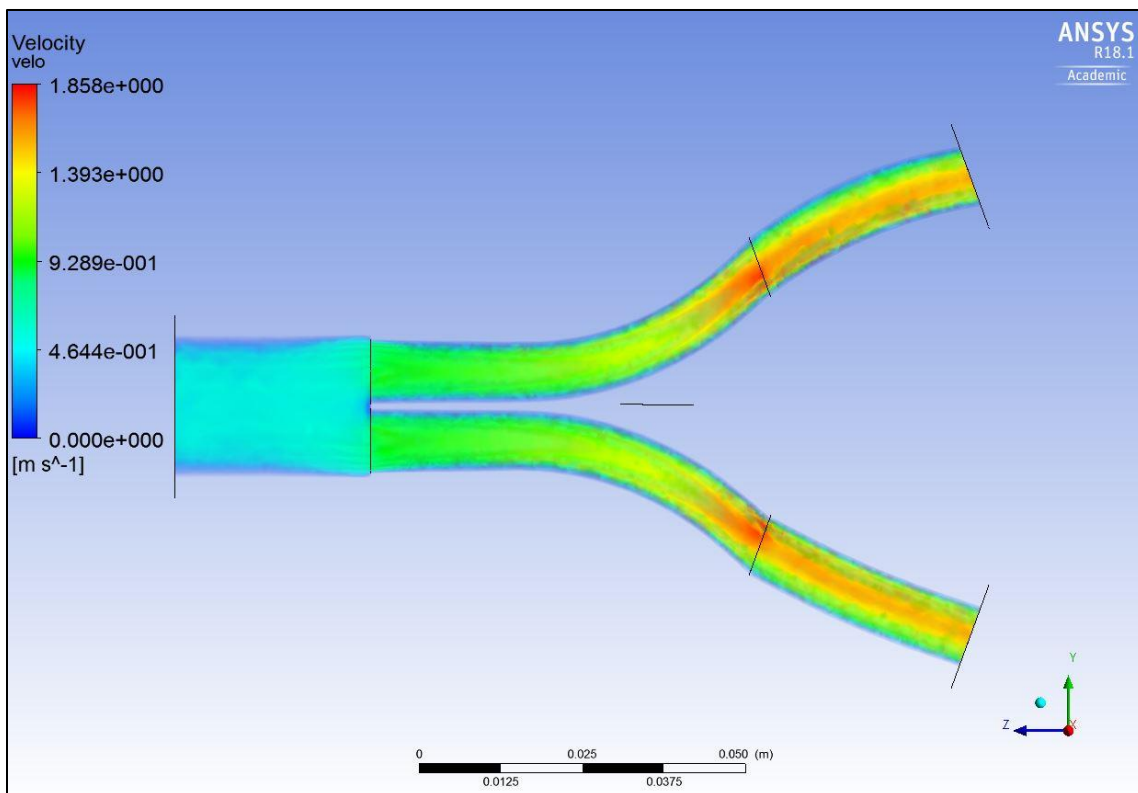


Figure 4.6 Model of the velocity contours of the kissing stent aortic bifurcation model.

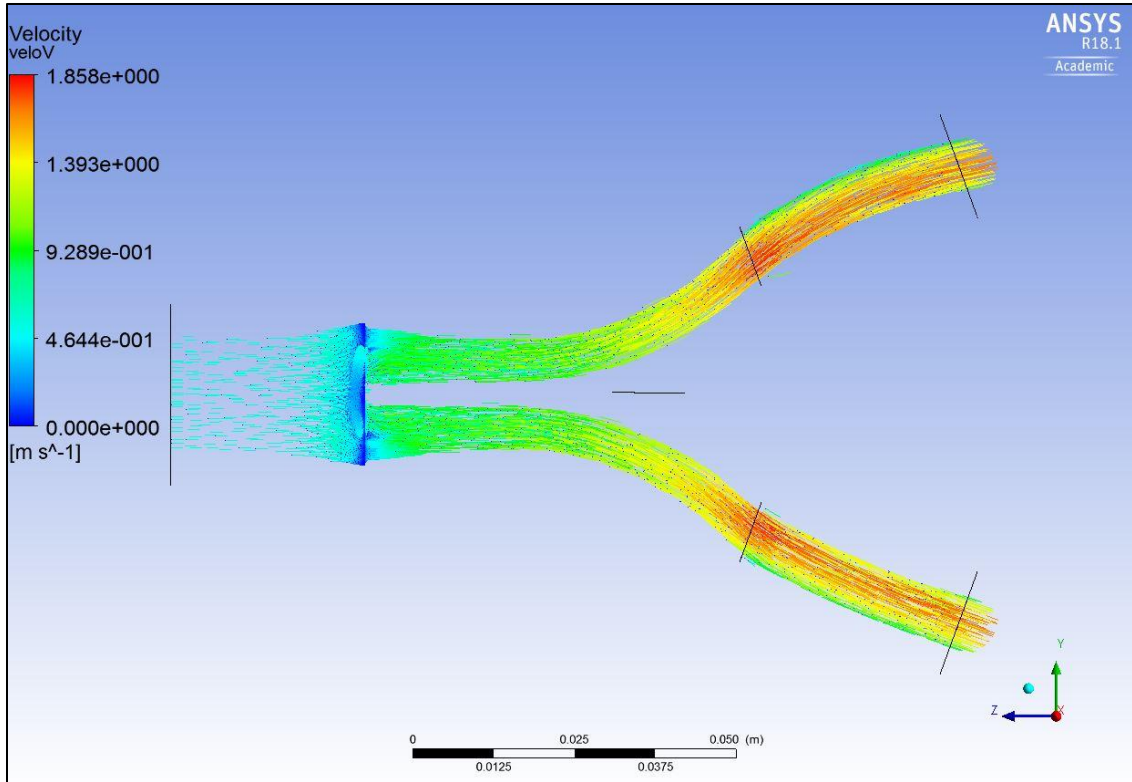


Figure 4.7 Model of the velocity vector map of the kissing stent aortic bifurcation model.

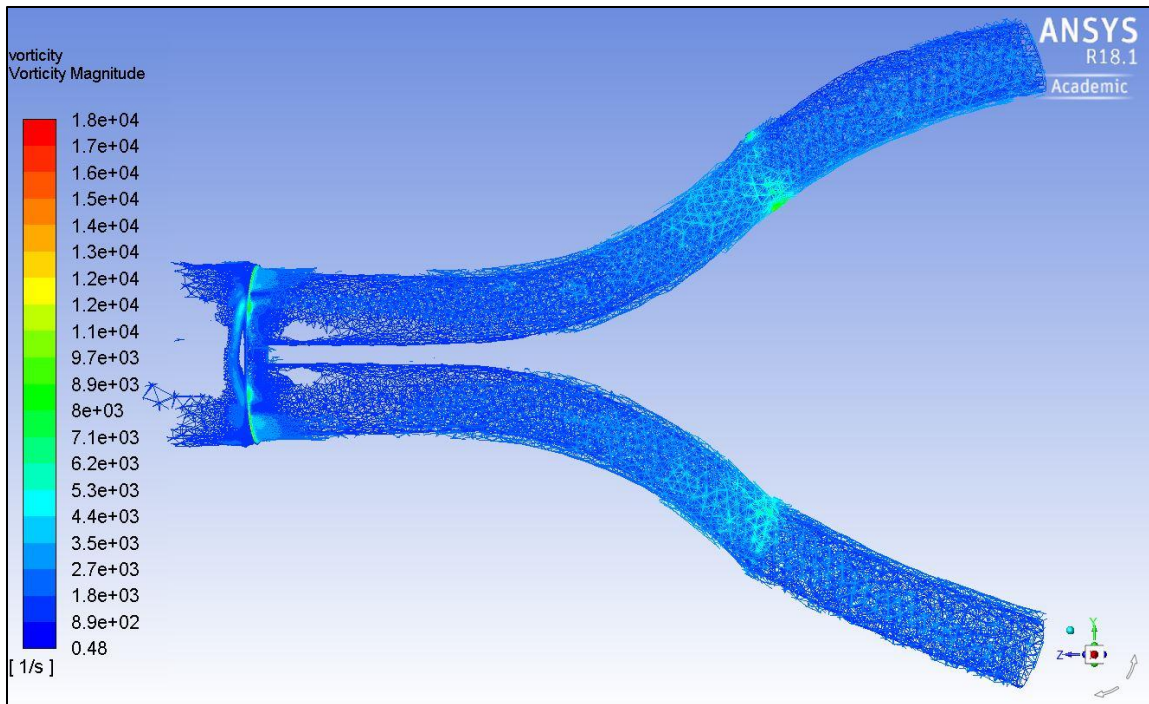


Figure 4.8 Model of the vorticity of the kissing stent aortic bifurcation model.

4.4 Proposed AIFEN Stent, 5mm Fenestration

The fenestrated arterial stenting procedure was studied as a potential intervention for aortoiliac occlusive disease. The stenting procedure with a 5mm fenestration in the ipsilateral main body (Fig. 4.9) was studied to observe the minimum size the fenestration should be modeled and to observe performance at this size. The velocity contours (Fig. 4.10) showed a maximum velocity of 3.36 meters per second due to the small fenestration, but did not show flow direction change (Fig. 4.11) when the image of the stent was superimposed over the flow field. Peak vorticity (Fig. 4.12) was discovered near the external outlet of the fenestration, primarily due to the changes in diameter in that space.

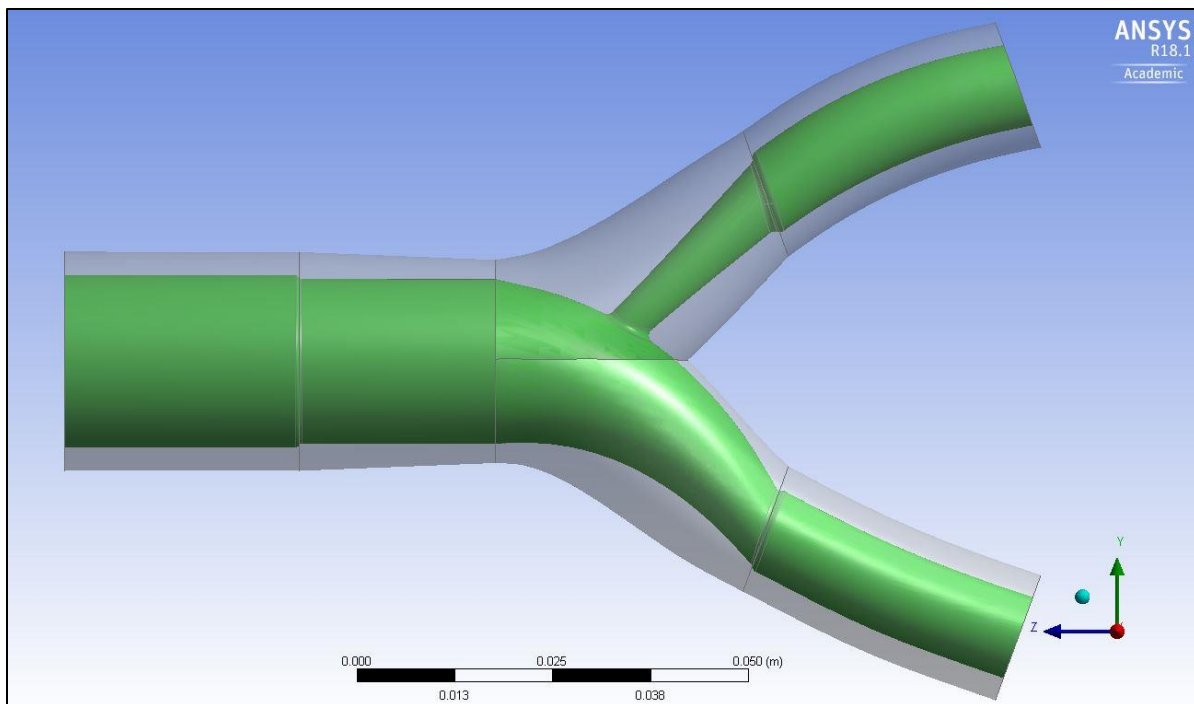


Figure 4.9 Model of the fluid fill of the ipsilateral main body stent aortic bifurcation model with a 5mm fenestration.

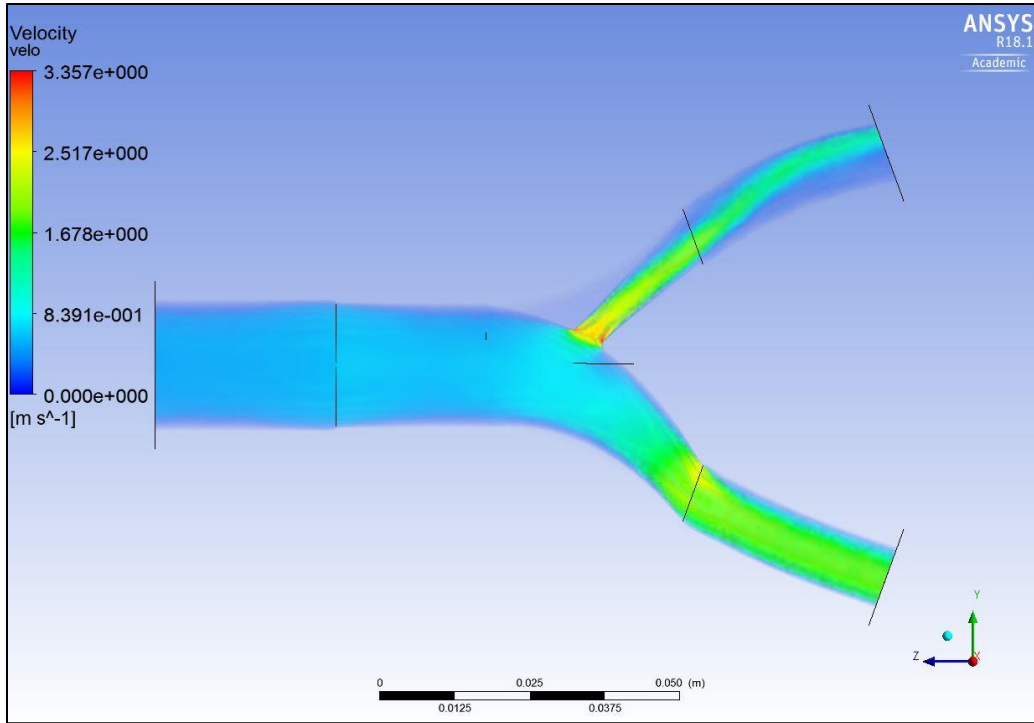


Figure 4.10 Model of the velocity contours of the ipsilateral main body stent aortic bifurcation model with a 5mm fenestration.

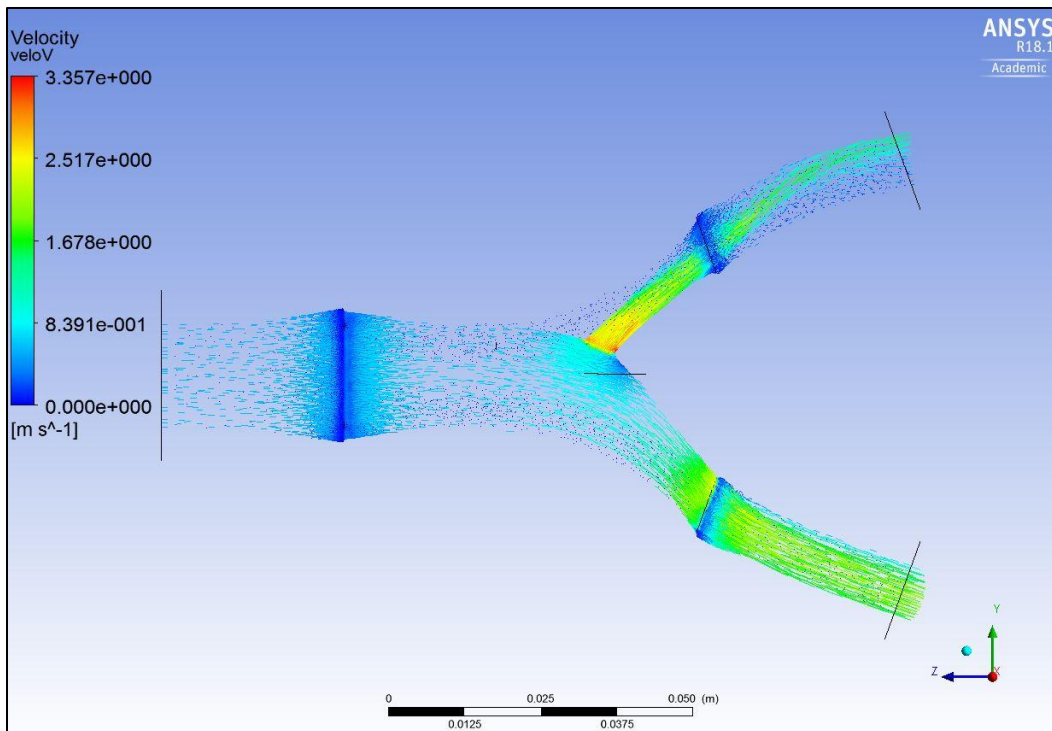


Figure 4.11 Model of the velocity vector map of the ipsilateral main body stent aortic bifurcation model with a 5mm fenestration.

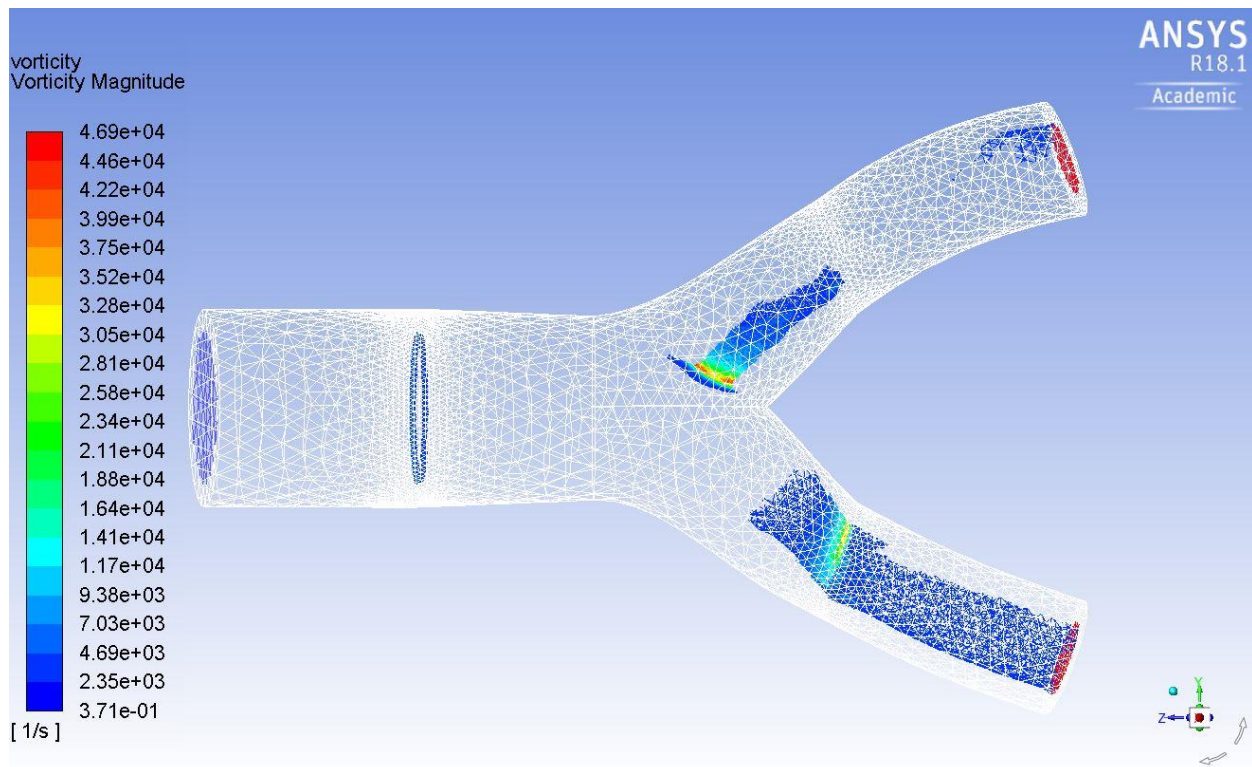


Figure 4.12 Model of the vorticity of the ipsilateral main body stent aortic bifurcation model with a 5mm fenestration.

4.5 Proposed AIFEN Stent, 10mm Fenestration

In addition to the 5mm fenestration, a 10mm fenestrated stenting procedure in the ipsilateral main body (Fig. 4.13) was studied to observe the median size the fenestration should be modeled to as well as observing performance at this size. The velocity contours (Fig. 14) showed a maximum velocity of 2.03 meters per second, a decrease after an increase in fenestration size, while also not showing any sign of stagnation (Fig. 4.15) when the image of the stent was superimposed over the flow field. Peak vorticity (Fig. 4.16) was discovered near the external outlet of the fenestration, however the maximum vorticity decreased in comparison to the previous 5mm fenestration model.

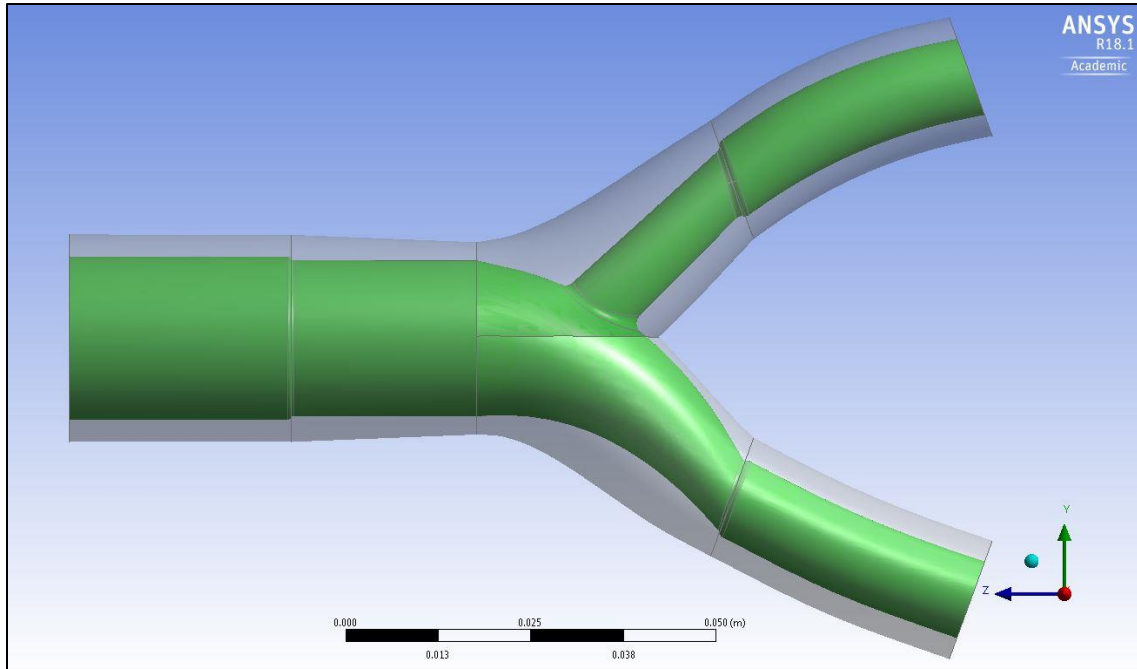


Figure 4.13 Model of the fluid fill of the ipsilateral main body stent aortic bifurcation model with a 10mm fenestration.

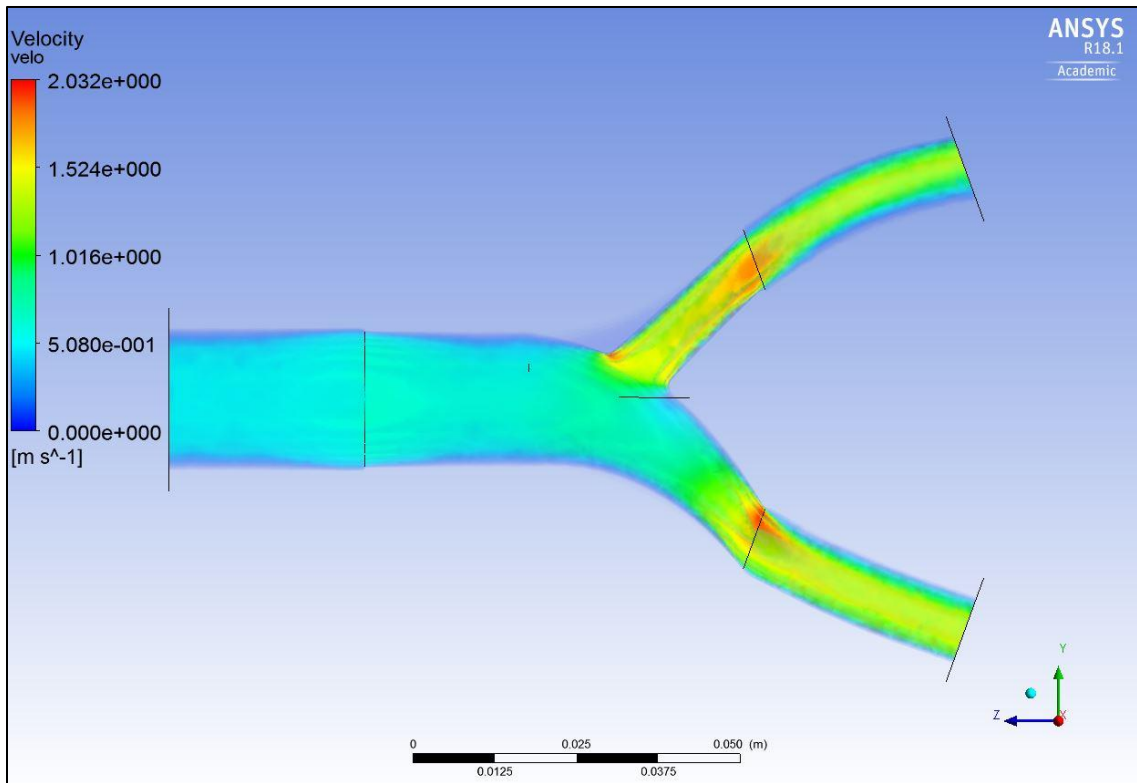


Figure 4.14 Model of the velocity contours of the ipsilateral main body stent aortic bifurcation model with a 10mm fenestration.

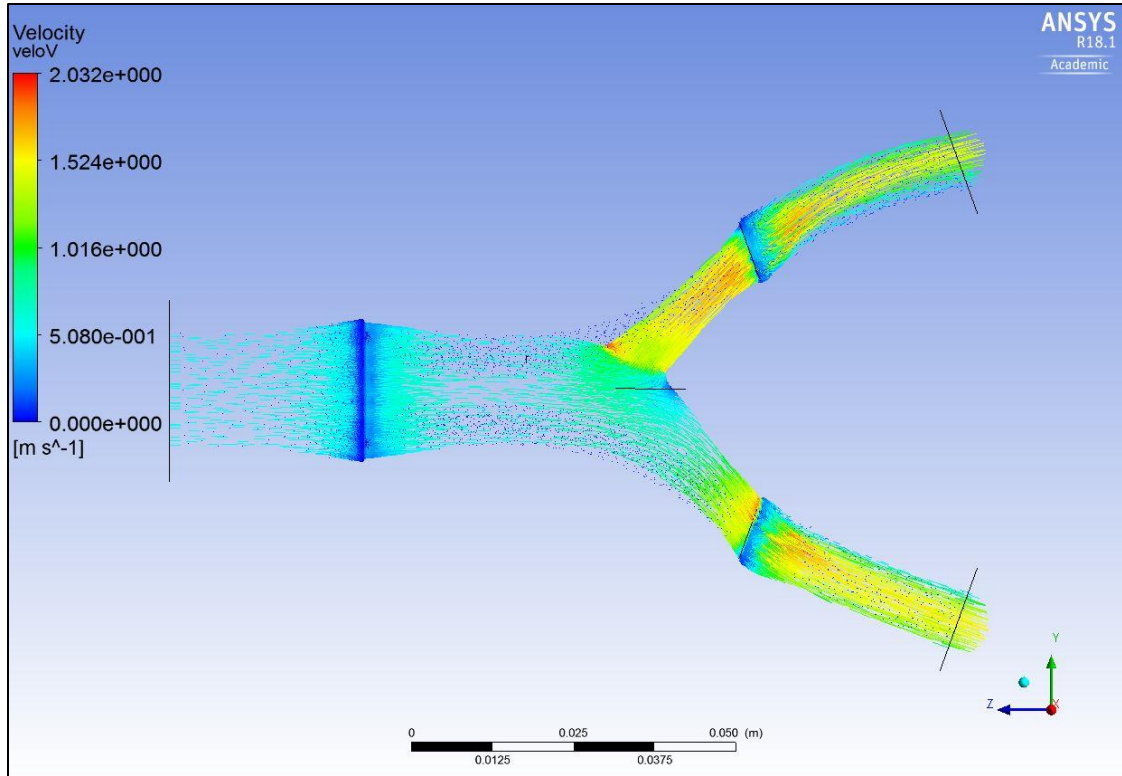


Figure 4.15 Model of the velocity vector map of the ipsilateral main body stent aortic bifurcation model with a 10mm fenestration.

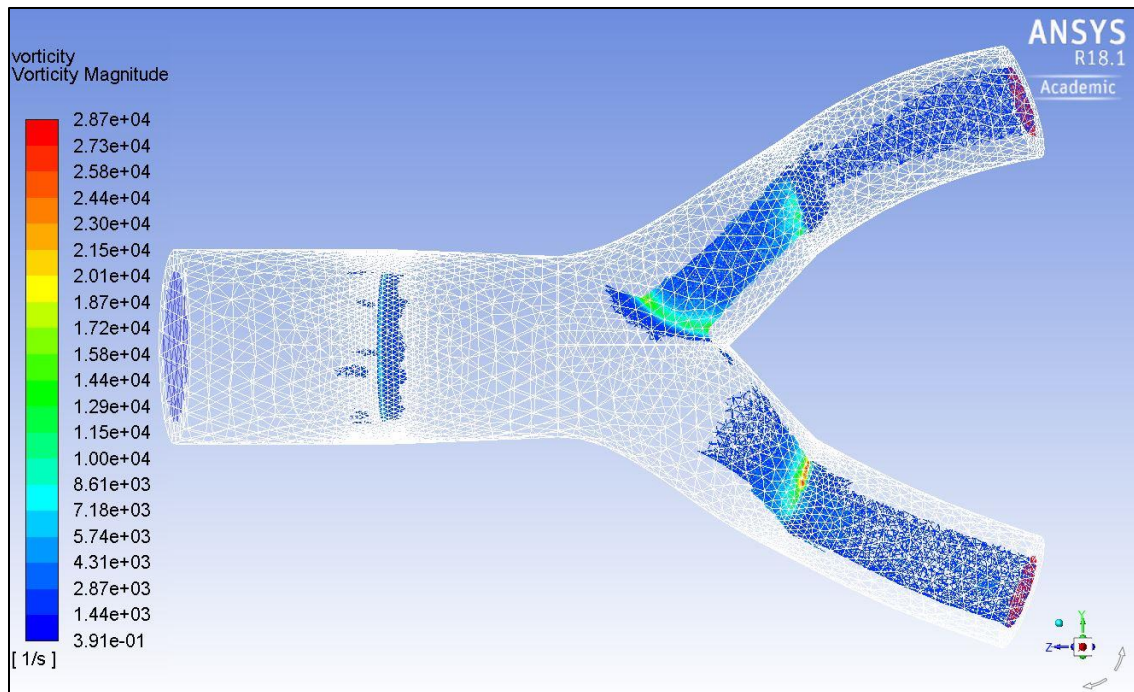


Figure 4.16 Model of the vorticity of the ipsilateral main body stent aortic bifurcation model with a 10mm fenestration.

4.6 Proposed AIFEN Stent, 15mm Fenestration

Lastly, a 15mm fenestrated stenting procedure in the ipsilateral main body (Fig. 4.17) was studied to observe the maximum size the fenestration should be modeled to as well as observing performance at this size. The velocity contours (Fig. 4.18) showed a maximum velocity of 2.44 meters per second, a decrease in velocity from the 5mm fenestration model after an increase in fenestration size, but an increase in velocity in comparison to the 10mm fenestration model. In addition, no sign of stagnation was observed (Fig. 4.19) when the image of the stent was superimposed over the flow field. Peak vorticity (Fig. 4.20) was discovered throughout the contralateral complementary iliac stent, most likely due to the tapered diameter.

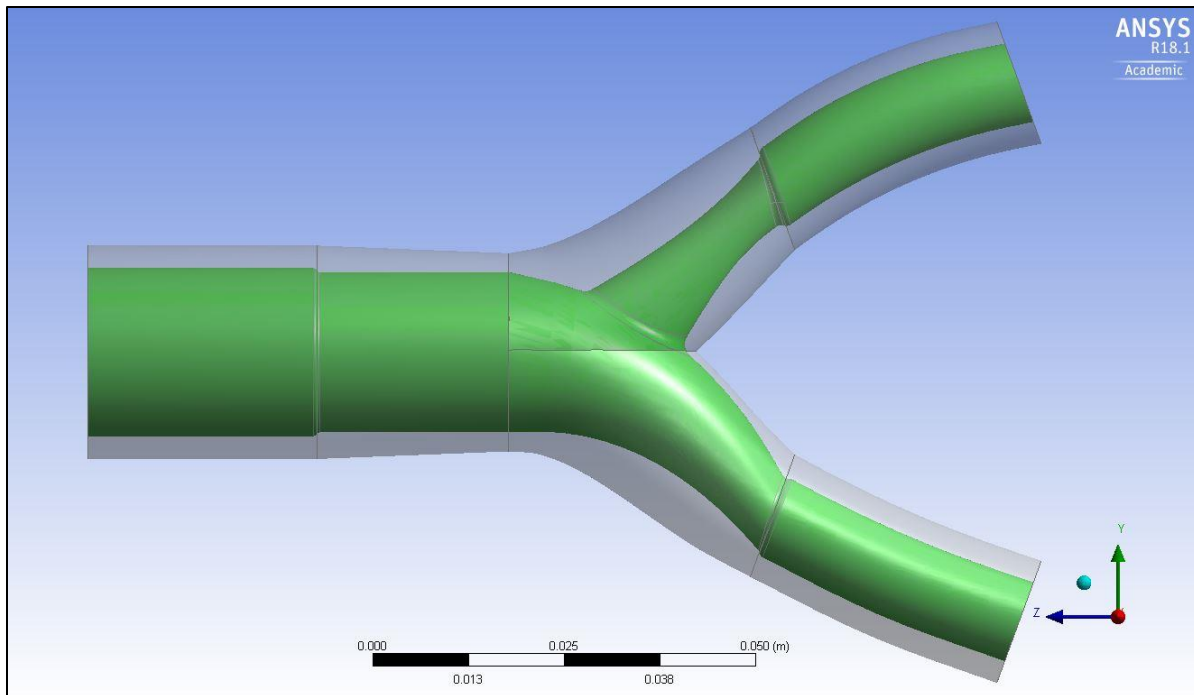


Figure 4.17 Model of the fluid fill of the ipsilateral main body stent aortic bifurcation model with a 15mm fenestration.

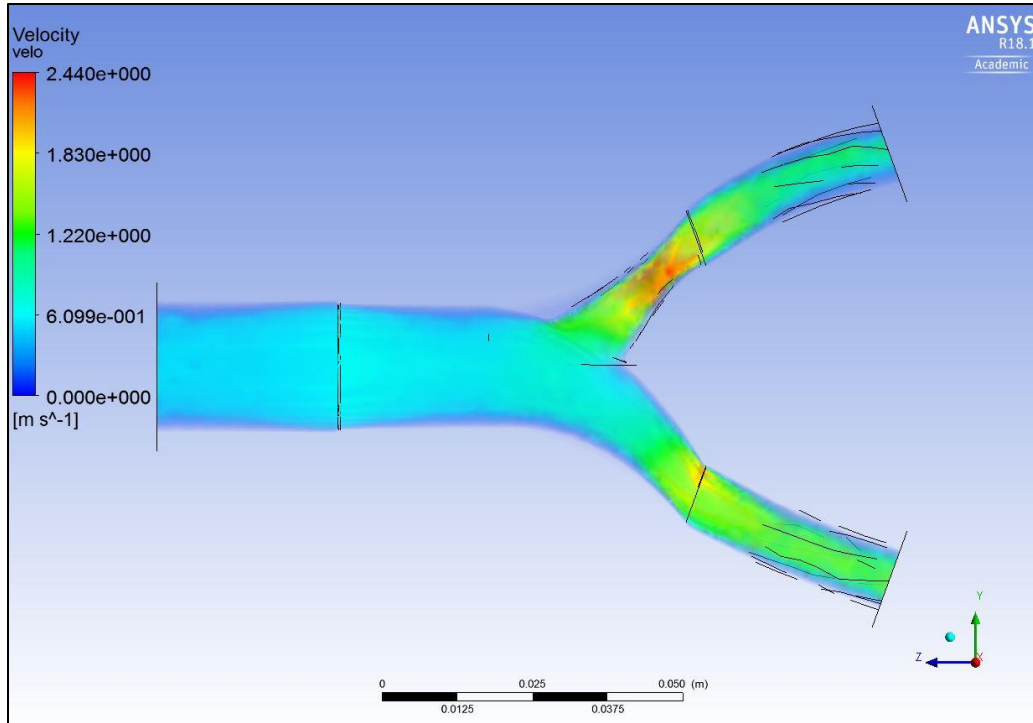


Figure 4.18 Model of the velocity contours of the ipsilateral main body stent aortic bifurcation model with a 15mm fenestration.

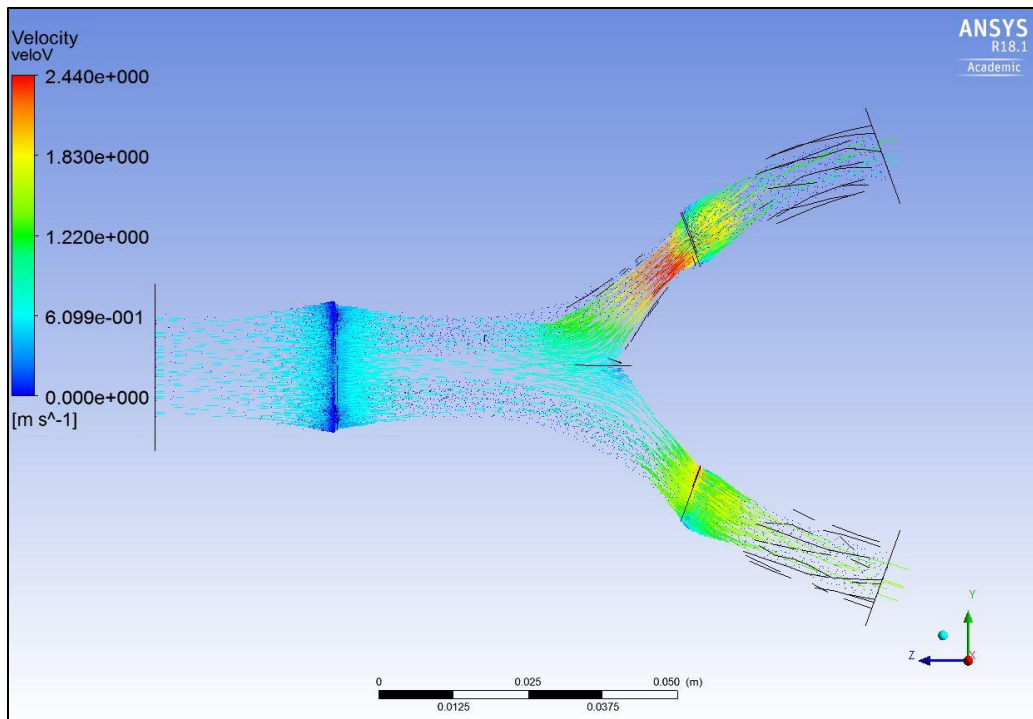


Figure 4.19 Model of the velocity vector map of the ipsilateral main body stent aortic bifurcation model with a 15mm fenestration.

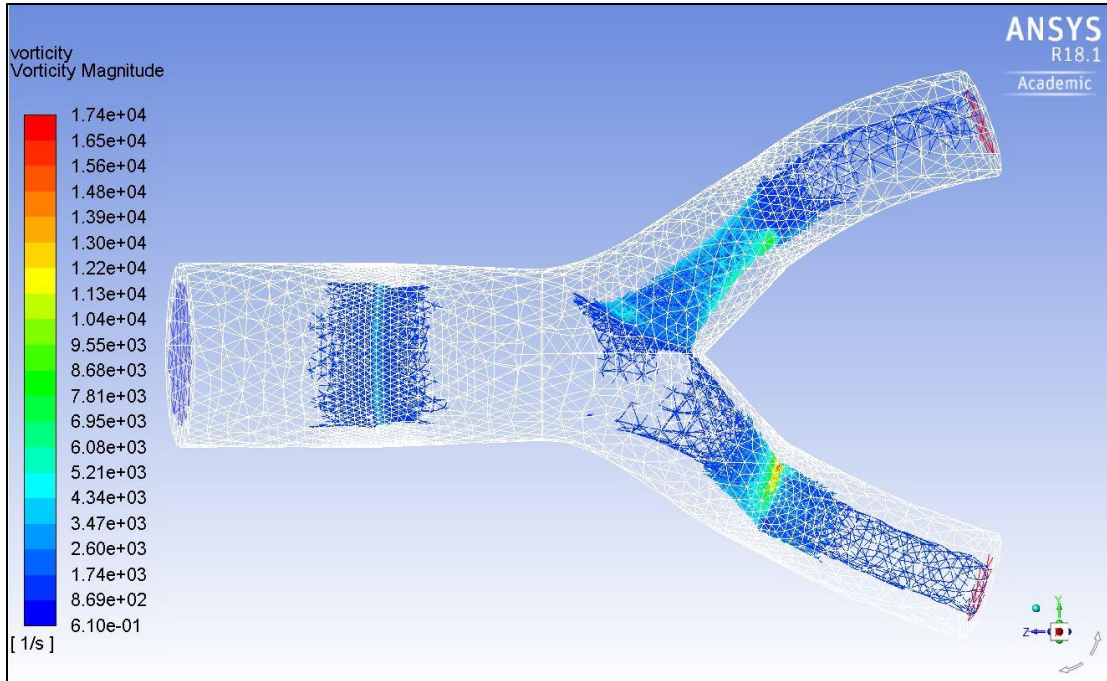


Figure 4.20 Model of the vorticity of the ipsilateral main body stent aortic bifurcation model with a 15mm fenestration.

4.7 Tabulated Data

Table 4.1 displays the extracted mass flow rate data from the all simulations in order to determine sufficient mass flow transfer from the distal aorta to the common iliac arteries. Note that outlet-1 is the common iliac artery exit that receives flow through the fenestration in the ipsilateral main body stent for the fenestrated stent models in particular.

Table 4.1 Table of average mass flow rates for all simulations.

	Inlet [kg/s]	Outlet-1 [kg/s]	Outlet-2 [kg/s]
Healthy Bifurcation	0.159	0.0787	0.0801
Unhealthy Bifurcation	0.0948	0.0466	0.0482
Ideal Kissing Stents	0.159	0.0791	0.0791
AIFEN Stent, 5mm	0.159	0.0423	0.117
AIFEN Stent, 10mm	0.159	0.0701	0.0886
AIFEN Stent, 15mm	0.159	0.0650	0.0932

Table 4.2 displays the extracted velocity data from the all simulations in order to determine sufficient flow of blood to properly match the healthy bifurcated. Note again that outlet-1 is the contralateral iliac artery for the fenestrated stent models, similar to Table 4.1.

Table 4.2 Table of average velocities for all simulations.

	Outlet-1 [m/s]	Outlet-2 [m/s]
Healthy Bifurcation	0.474	0.456
Unhealthy Bifurcation	1.01	0.990
Ideal Kissing Stents	0.567	0.539
AIFEN Stent, 5mm	0.258	0.708
AIFEN Stent, 10mm	0.413	0.539
AIFEN Stent, 15mm	0.186	0.318
*Average Velocity for all Inlets: 0.2264 m/s		

Chapter 5

Discussion

5.1 Mass Flow Rate

Mass flow rate was extracted from each simulation in order to evaluate the ability of each stenting procedure to evenly distribute blood flow into each common iliac artery. Typically, a normal aortic bifurcation would be expected to evenly distribute the amount of blood that flows into each common iliac, so ideal results are expected to have common iliac mass flow rates that are nearly half of the inlet mass flow rate in the distal aorta. In these symmetrical models of healthy, unhealthy, and kissing stent aortic bifurcations, the distribution was even. Likely due to the minor asymmetry and rigid analysis, the fenestrated stent models have minor error in distributing blood flow. The mass flow rate was 46.5% different between the contralateral common iliac artery and the collateral common iliac artery for the 5mm fenestration model, which equates to a 23.1% mass shift in blood overall. This amount of error would be deemed unacceptable to treat the aortic bifurcation, thus providing some evidence that a 5mm fenestration is too small. For the 10mm fenestration model, a mass flow rate error of 11.3% was found between the contralateral common iliac artery and the other common iliac artery, which equates to a 5.01% shift in blood mass. The results are much more ideal for this preliminary analysis of the fenestrated stent and is more reasonable for the patient. For the 15mm fenestration model, a mass flow rate error of 17.8% was found between the contralateral common iliac artery and the other common iliac artery, which equates to a 9.12% shift in blood mass. While this result is superior to the 5mm fenestration model, a mass shift close to 10% is not ideal for the health of the patient. Overall, the 10mm model shows the most potential among the three fenestration trial models, and decreasing this percentage can be achieved by tailoring the diameters of the two arms of the fenestrated stent as well as the angle of approach for the fenestration itself.

5.2 Average Outlet Velocity

Velocity is a key parameter in evaluating performance of these cardiovascular stents. The cardiac cycle was modeled by a boundary condition of the blood velocity boundary consisting of a half-sinusoid that ranged from 0.1 meters per second to 0.6 meters per second with an average of 0.226 meters per second (see Fig. 2.6 and the appendix).

In order to establish that the simulated data was reasonable, the maximum Reynold's number for fluid flow in a pipe-like structure was recorded for each simulation. Reynold's numbers of 350, 453, and 488 were found for the preceding simulations of the healthy bifurcation, unhealthy bifurcation, and ideal kissing stents procedure, respectively. Reynold's numbers of 594, 488, and 891 were found for the proposed AIFEN stent procedures with a 5mm fenestration, 10mm fenestration, and 15mm fenestration, respectively. Because all of these values are far less than 2,000, it is safe to assume that all fluid flow in this thesis is laminar. However, an argument can be made about the higher values in both the AIFEN stenting procedures with 5mm and 15mm fenestrations. Because of the similar results found in the mass flow rate analysis and the later velocity analysis, it is understandable that these fenestrated models are providing higher Reynold's number due to unideal conditions. This is most likely due to the tapered nature of the complementary contralateral iliac stent and the increase in flow velocity that it produced.

It was observed that these initial boundary condition velocities were accelerated by the narrowing of the aortic bifurcation, as velocity is expected to increase when flow enters an area with a smaller diameter. For the healthy aortic bifurcation model, which was symmetrical, the average velocities of over the two outlets were between 0.456 and 0.474 meters per second for the collateral and contralateral outlets, respectively. Because of the symmetry, the difference between these represents the numerical error of less than 3% over a cardiac cycle. The outlet velocities in the unhealthy aortic bifurcation model were nearly double this, ranging between 0.990 and 1.01 meters per second for the collateral and contralateral outlets, respectively, representing error of less than 2%. These results establish a fundamental range of physiological to pathophysiological velocity fields with which to assess the two arterial stenting designs.

The aortic bifurcation modeled with the kissing arterial stenting procedure decreased outlet velocity in comparison to the unhealthy aortic bifurcation, with average velocities of 0.567 and 0.539

meters per second for the collateral and contralateral outlets, respectively, but did not decrease these to the levels of the healthy aortic bifurcation model. The 10mm fenestrated stent model lead to much more efficient outlet velocities, with average velocities 0.413 m/s and 0.539 m/s for the collateral and contralateral outlets, respectively. Due to the contours of the 10mm fenestrated stent model, the collateral iliac artery results in an outlet velocity nearly equivalent to the healthy aortic bifurcation results, where the collateral iliac artery outlet velocity is similar, but slightly superior, to the results of the kissing arterial stenting procedure.

Unlike the ideal results from the 10mm fenestration model, the 5mm and 15mm fenestration model resulted in poor velocity results at each iliac outlet. The average velocity resulted in 0.258 m/s and 0.708 m/s for the 5mm fenestration model and 0.186 m/s and 0.318 m/s for the 15mm fenestration model for both the collateral and contralateral iliac artery outlets, respectively. Ultimately, these are unrealistic results in matching the blood flow velocity of a healthy aortic bifurcation. An observation is that the contralateral complementary iliac stent, in both the 5mm and 15mm fenestration models, is tapered to match the expected diameter of the common iliac vessel. It appears that the flux of diameter changes from the fenestration outlet, throughout the complementary iliac stent, and the common iliac artery itself may cause unideal conditions for the blood flow. The 10mm fenestration model produced results superior to the kissing stents procedural model, which did not include nearly any taper in the complementary iliac stent. Therefore, it should be concluded that, to achieve ideal conditions, keeping the contralateral iliac stent at a constant diameter is preferred.

The attenuated peak velocities in the 10mm fenestrated stent model are favorable and suggest that the design is worth of further investigation. A limitation that must be considered is the distortion of the bifurcation during heart palpitation was not modeled in this study. However, from these results, it can be concluded that the design of the fenestrated stent provides a smooth transition of blood flow in the bifurcation from the distal aorta to the common iliac arteries. Provided that pressure is maintained throughout the aortic bifurcation model, this reduction in peak average velocity is consider a favorable outcome for the design of the fenestrated stenting procedure, in favor of the 10mm model, over the kissing arterial stenting procedure. However, because these velocities values are lower than expected from the literature, further analysis is warranted. [22]

5.3 Velocity Contour and Vector Plots

Due to meshing and modeling conditions, CFD simulations occasionally predict anomalously larger velocities, pressures, and other field variables at sharp corners and quick changes in diameter. To avoid potential artifacts like this, a careful analysis was done to observe the velocity and vorticity contour plots. This enabled determination of whether stagnation or undesirable flow occurred along the length of the bifurcation model.

The healthy aortic bifurcation, in Fig. 4.2, showed a gradual velocity towards the center of the vessel near 0.6 meters per second in the distal aorta. This matches the blood flow inlet function that has a peak velocity around approximately 0.6 meters per second. The model shows a steady increase in velocity to approximately 1 meter per second in the common iliac arteries, closely matching the literature. [22] Additionally, zero velocity was seen at the walls due to the set boundary condition. No reverse flow (negative velocities) were observed, meaning that no flow separation or turbulence occurred.

The unhealthy aortic bifurcation model, in Fig. 4.4, performed nearly identically to the healthy aortic bifurcation model. However, using the velocity color scale to evaluate the magnitude of the velocities, there was a small increase in velocity in the distal aorta in comparison to the healthy bifurcation model. The common iliac arteries show a velocity flow that is over double that of the healthy bifurcation. These results are expected as the unhealthy bifurcation has inner diameters that are nearly half of the healthy bifurcation. The rigid assumption of these vessels could have possibly impacted velocity as, normally, some of this energy would be transferred to the arteries themselves.

The kissing stent aortic bifurcation velocity contour plot, in Fig. 4.6, shows a gradual velocity a bit less than what is expected in the distal aorta. This is possibly due to the sudden change in cross-section due to the kissing stent inlet. Using the color velocity scale as a guide, the inlet of the two kissing stents showed a rapid increase in velocity in each stent and even more of a velocity increase at the outlet of each artery. There was also a particularly large radial spread in velocity in the distal iliac vessels. These large jumps in velocity are considered to be suboptimal and can introduce unwanted stress in the aortic bifurcation. In terms of velocity direction, Fig. 4.7 showed a few velocity disturbances in the kissing stent aortic bifurcation model. Most notably, the disturbance around the entrance of the kissing stents shows stagnation and backflow of the blood. An image of

this disturbance can be seen in Fig. 5.1. In this figure, blood flow in the distal aorta is impacted by the abrupt surface that the kissing stents create due to the presence of two new inlets with no smooth transition. This results in the collection of flow around the edge of the kissing stent inlets, stagnation at the outer edge of the distal aorta at this location, and backflow to allow flow into each kissing stent inlet.

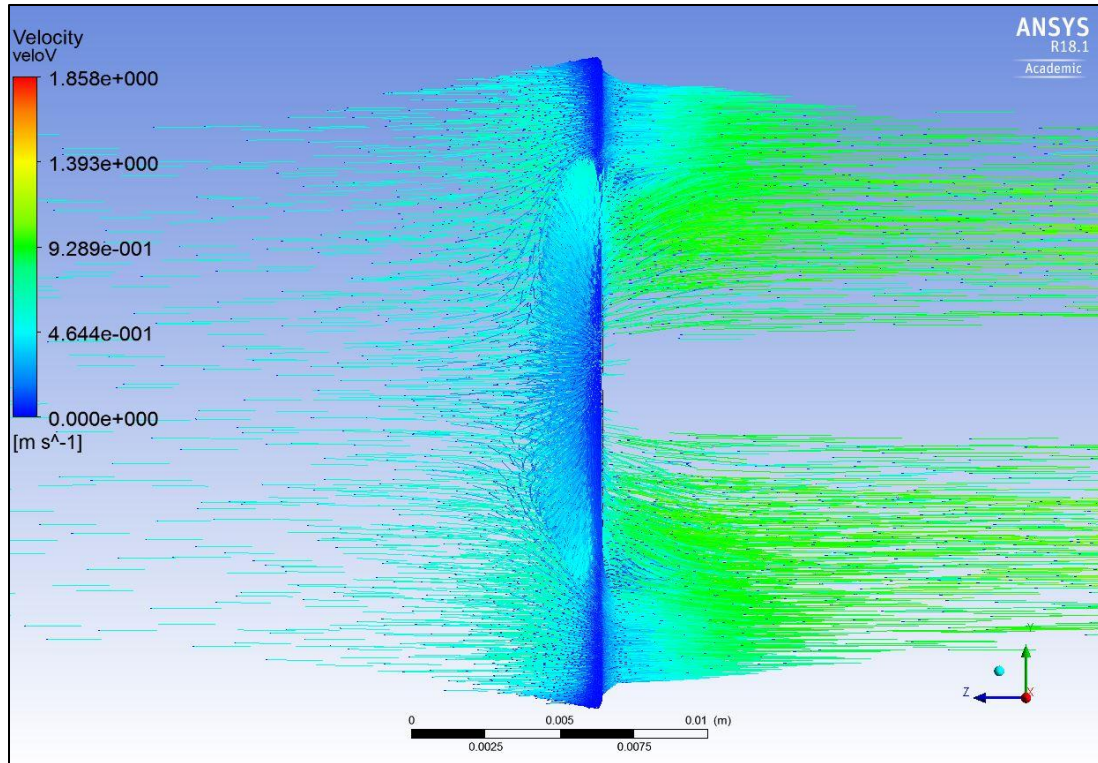


Figure 5.1 Zoomed in model of the velocity vectors of the kissing stent aortic bifurcation model. The image depicts the inlet of the two kissing stents in the distal aorta.

These drawback to the kissing stent design are not artifacts of the modeling. The modeling of the kissing stent inlet in the distal aorta, if anything, attenuated the propensity for such artifacts. Typically, the stents crush and press plaques present up to the vessel walls to create new lumens for blood flow. However, kissing stents typically leave gaps where the two stents touch in the distal aorta. Blood flow in these gaps causes significant thrombus formation in the bifurcation. In this study, the plaque was assumed to fill these gaps and form a solid barrier around the two kissing stents. This should attenuate backflow in the model. Even with this attenuation, back flow still occurred, as seen in Fig. 5.1. This backflow is a significant disadvantage to treatment using the kissing stent method and will certainly results in thrombosis.

The fenestrated stent models showed flow fields that were free of deleterious features. The gradual velocity in the distal aorta was similar to the healthy aortic bifurcation model and the transition of velocity into the stent was constant. These results already show an improved resultant flow at the inlet of the stent. Blood flow was less radially distributed in the common iliac vessels and suitable velocities nearly equivalent to the healthy bifurcation model were observed, especially with the ideal 10mm fenestration model. The most notable result is that no stagnation is observed in any of the fenestrated stent models, seen in Fig. 4.11, 4.15, and 4.19. This is most likely due to the design of the device to have only one stent exist in each vessel cross-section at one time. Additionally, the stents are flared together, which eliminates any potential for low velocity areas, which can be seen in a preliminary test in Fig. 5.2.

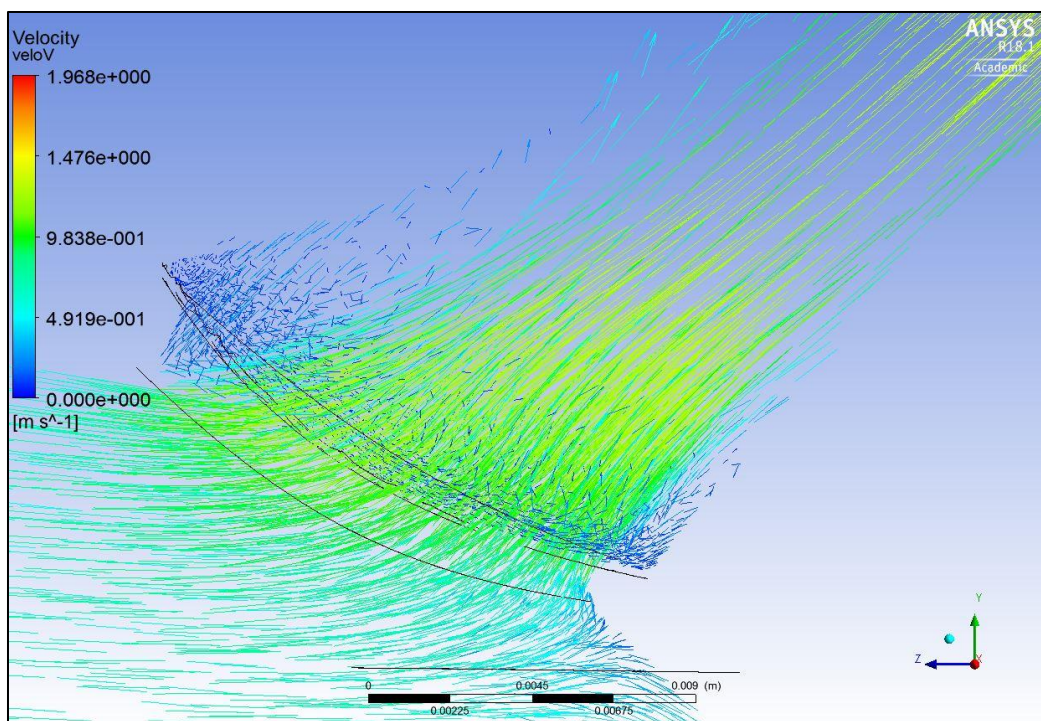


Figure 5.2 Zoomed in model of the velocity vectors of an early fenestrated stent design. This image represents what happens when the stents are not flared together, where the iliac stent can decompress to a maximum diameter larger than the existing fenestration. The external edges of the fenestration show mixing and slow-moving blood flow that will cause thrombosis to occur.

Looking at the three fenestration models in particular, the 5mm model included some notable problems. The characteristics of the blood flow that moves through the entirety of the ipsilateral main body stent are very ideal, as seen in Fig. 4.10. The flow in the distal aorta is maintained around expected values in literature and transitions well to the collateral common iliac

artery with no disturbances. It is, however, the contralateral iliac artery results that make this fenestration inadequate. The velocity of the flow spikes near the edges of the fenestration, where the complementary stent is flared, and causes radially unbalanced flow in the common iliac artery. While a single side of the model matches the healthy bifurcation more than the kissing stents could, the contralateral results are enough to reject any potential for a 5mm fenestration. On the fenestration maximum size, the 15mm fenestrated model also produced interesting results. Similarly to the 5mm model, ideal conditions are seen moving throughout the ipsilateral main body aortoiliac stent, while the contralateral iliac artery produces concerns, as seen in Fig. 4.18. While there is less of a spike in velocity at the fenestration itself, the velocity nearly maxes out at the outlet of the contralateral complementary iliac stent. It appears that the flow stabilizes, however this high of a blood flow velocity nearly matches unhealthy conditions, making this an unideal result. Lastly, the 10mm fenestration produced more optimal results in this preliminary study of the AIFEN stent. Correspondingly to the previous 5mm and 15mm fenestration models, the blood flow results are representative of ideal conditions when moving throughout the ipsilateral main body aortoiliac stent, as seen in Fig. 4.14. It should be noted that there are a few spikes of velocity concentrated near outlets of the stents, which can be produced by sharp corners in the CAD model in rigid conditions. These concentrated results are unrealistic of the aortic bifurcation, so skewed maximum values of velocity have been taken into account and disregarded. The flow transitions very well into the complementary iliac stent, nearly representing healthy condition in the common iliac vessels. A zoomed in model of this transition can be seen in Fig. 5.3. Nearly exact velocities would be hypothesized in the common iliac vessel once the fenestration is tailored more to fit the direction of flow. The CAD models were designed to have a fenestration that faced the same direction of the angle each iliac artery was modeled from. If the angle of the fenestration itself is more appropriated to the approach of blood flow in the distal aorta, in tandem with the 10mm results from this thesis, healthy conditions in the entire aortic bifurcation can be achieved. This suggests that the fenestrated stent technique, particularly with a 10mm fenestration, is more suitable for treating the aortic bifurcation than the kissing stent technique.

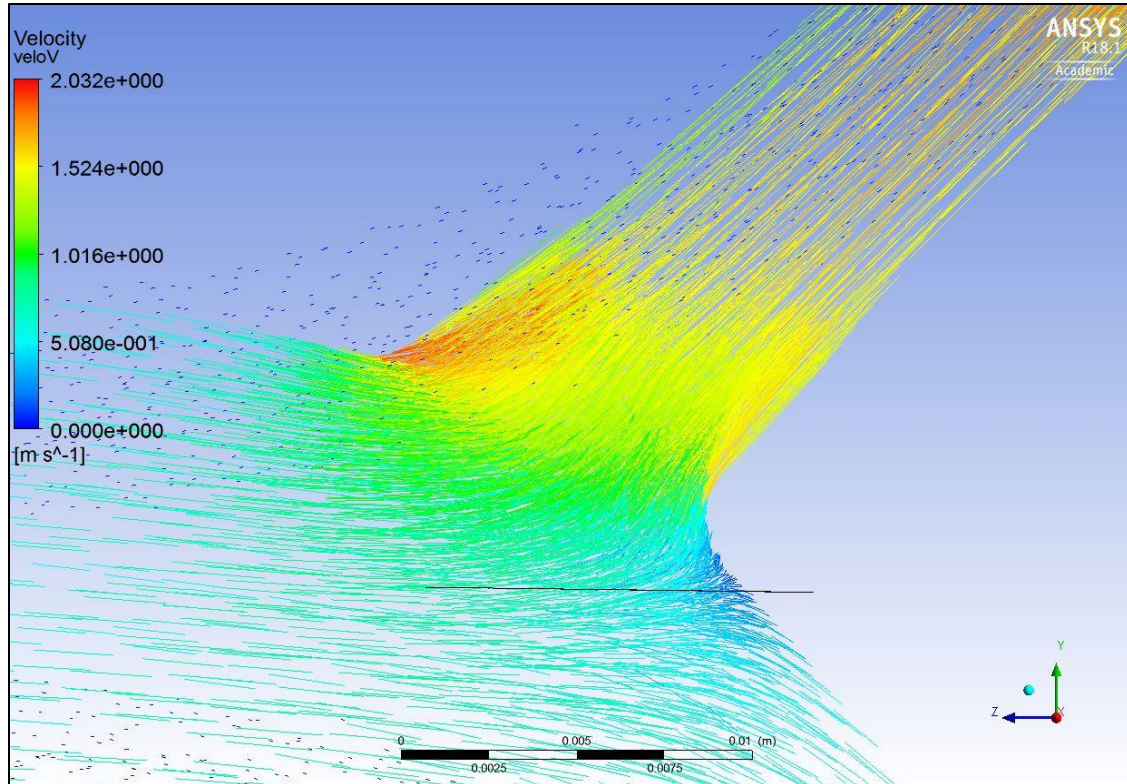


Figure 5.3 Zoomed in model of the velocity vectors of the ipsilateral main body stent aortic bifurcation model with a 10mm fenestration. The image depicts the exit of the fenestration into the common iliac artery.

5.4 Vorticity

Vorticity contour plots were also extracted in an additional attempt to verify if any turbulence or stagnation was occurring in the simulated models, particularly in the stented aortic bifurcation models. For the healthy and unhealthy aortic bifurcation models, vorticity conditions were trivial. Because of the smooth surfaces and symmetric modeling, no focal points of vorticity were found and the values found in the results represent the potential of vorticity due to the varying values of velocity between each model.

Examining the vorticity of the kissing stent treated aortic bifurcation model, in Fig. 4.8, revealed fields that were less uniform than observed the in healthy and unhealth aortic bifurcation models. Peak values, in units of radians per second, were observed with focal points at the inlets and outlets of the stents. These were at locations similar to where issues were observed in the velocity contour plot. Because a lot of vorticity is focused at the inlet surface, and because of the reverse

direction of flow at this inlet, thrombosis of blood would be expected to exist here. This furthermore confirms the hazards that the inlet of the kissing stent procedure produces.

The fenestrated stent-treated aortic bifurcation models also show signs of vorticity. Observing the vorticity of the 5mm fenestration model first, in Fig. 4.12, points of vorticity only exist at the inlets of outlets of the stents. For this model, a large amount of vorticity can be found around the external edge of the fenestration in the ipsilateral main body stent, likely due to the difference in diameter sizes causing blood flow to accelerate. Residual effects of the radially unbalance flow can also be seen near the end of the contralateral common iliac artery. Observing the 15mm fenestration model for vorticity, in Fig. 4.20, points of vorticity are focused in a similar fashion to the 5mm fenestration model. Additionally, larger values of vorticity exist in the complementary common iliac stent where the iliac stent tapers down to fit the expected size of the common iliac vessel. Lastly, the ideal 10mm fenestrated model show sufficient results over both the 5mm and 15mm fenestration models, in addition to the kissing stent procedural model, as seen in Fig. 4.16. This is because significant portions of vorticity are reduced in the complementary common iliac vessel and at the inlet of the ipsilateral main body stent suggesting that the 10mm fenestration design is a substantial improvement over the current standard of care.

Chapter 6

Conclusion

6.1 Summary of Results

Using models of the healthy and unhealthy aortic bifurcation to establish a fundamental range of acceptable values and outcomes, it was shown that significant design progress was made over the kissing stents angioplasty method with a novel fenestrated stent angioplasty treatment option. With computer-aided design models and a fluid simulation of non-Newtonian blood pulsating flow, evidence is clear that improved treatment options exist for aortoiliac occlusive disease. The most significant evidence of superiority of the proposed fenestrated stent treatment method was in the velocity contour plots and velocity vector maps of each aortic bifurcation simulation. Substantial issues such as stagnation, high velocities, and back-flow are involved the common kissing stent angioplasty technique, and these issues are eliminated in the proposed fenestrated stent design, in favor of the 10mm fenestration model. Therefore, this new fenestrated stenting technique of the aortic bifurcation now shows clear potential for superior performance in treating a serious and life-threatening disease.

6.2 Future Work

Optimization of the proposed fenestrated stent is still needed in order to maximize the potential of the medical device. The fenestration, in particular, should be the focal point of next-phase design aims. This fenestration must allow a more evenly distributed mass blood flow from the distal aorta to both of the common iliac arteries. Additionally, a smoother transition of blood into the fenestration will decrease the likelihood of possible high velocity focal points around the external edge of the fenestration in the contralateral common iliac artery. Further analysis will incorporate deformable bodies that will allow for a more realistic response from the aortic bifurcation as well. With a more optimized method of blood flow transition to the contralateral common iliac artery, this stent will be sufficiently prepared for final design steps and implementation into the surgical industry.

Appendix

MATLAB Description of Inlet Blood Pumping

The following MATLAB code describes the function inputted into the inlet of the distal aorta for all simulations. This function was rewritten to a proper file type to work with ANSYS Fluent.

```
% Time Span of Simulation, 10 Seconds
time = linspace(0,10);

% Constant obtained via Fourier Series
A0 = 2.094;
A1 = -1.121;
A2 = -0.3412;
A3 = -0.2507;
A4 = -0.1012;
A5 = -0.06782;
A6 = -0.04863;
A7 = -0.03503;
A8 = -0.02637;
B1 = 0.3113;
B2 = -0.2101;
B3 = 0.02114;
B4 = 0.00658;
B5 = 0.0001719;
B6 = 0.004727;
B7 = 0.005966;
B8 = 0.00664;
w = 120.51;

% Function
blood_velocity = (.6/3.3)*(A0 + A1*cos(time*w) + A2*cos(2*time*w) +
A3*cos(3*time*w) + A4*cos(4*time*w) + A5*cos(5*time*w) + A6*cos(6*time*w) +
A7*cos(7*time*w) + A8*cos(8*time*w) + B1*sin(time*w) + B2*sin(2*time*w) +
B3*sin(3*time*w) + B4*sin(4*time*w) + B5*sin(5*time*w) + B6*sin(6*time*w) +
B7*sin(7*time*w) + B8*sin(8*time*w));
```

References

- [1] Bean W. J., et. al. "Leriche Syndrome: Treatment with Streptokinase and Angioplasty." *American Roentgen Ray Society*. 1985.
- [2] Ku D. N., Giddens D. P., Zarins C. K., Glagov S. "Pulsatile flow and atherosclerosis in the human carotid bifurcation. Positive correlation between plaque location and low oscillating shear stress." *Arteriosclerosis, Thrombosis, and Vascular Biology*. Vol. 5,3. p. 293-302. 1985.
- [3] Rothwell P.M., Howard S.C., Spence J.D. "Relationship Between Blood Pressure and Stroke Risk in Patients With Symptomatic Carotid Occlusive Disease." *Stroke*. Vol. 34,11. p. 2583-2590. 2003.
- [4] Nagarsheth K.H., Rowe V.L., et. al. "Aortoiliac Occlusive Disease." *Medscape*. 2017.
- [5] Wholey M.H., Wholey M.H., Jarmolowski C.R. "Endovascular Stents for Carotid Artery Occlusive Disease." *Journal of Endovascular Therapy*. Vol. 4,4. p. 326-338. 1997.
- [6] Roger V.L., Go A.S., Lloyd-Jones D.M., et. al. "Heart Disease and Stroke Statistics 2011 Update: A Report From the American Heart Association." *Circulation* 2011; 123:e18-e209.
- [7] Mahoney, M.R. "Analysis of a Cardiovascular Stent in Balloon Angioplasty." *Cornell University: Confluence*. 2015.
- [8] Suwaidi J.A., et. al. "Immediate and long-term outcome of intracoronary stent implantation for true bifurcation lesions." *Journal of the American College of Cardiology*. Vol. 35,4. p. 929-936. 2000.
- [9] Uhl C., Betz T., Weiss B., Töpel I., Steinbauer M. "Results of hybrid procedures for treatment of aortoiliac Trans-Atlantic Inter-Society Consensus II D lesions with self-expanding covered heparin-bonded stent grafts." *The Journal of Cardiovascular Surgery*. DOI: 10.23736/S0021-9509.18.10295-3. 2018.
- [10] De Vries, S.O., Hunink, M.G.M. "Results of aortic bifurcation grafts for aortoiliac occlusive disease: A meta-analysis." *Journal of Vascular Surgery*. Vol. 26,4. p.558-569. 1997.
- [11] Wiskirchen J., Venugopalan R., Holton A.D., König C., Kramer U., Trübenbach J., Tepe G., Claussen C.D., Duda St.H. "Radiopaque markers in endovascular stents--benefit and potential hazards." *Georg Thieme Verlag Stuttgart: New York*. 2003.
- [12] Ouriel K., Veith F.J., Sasahara A.A. "A Comparison of Recombinant Urokinase with Vascular Surgery as Initial Treatment for Acute Arterial Occlusion of the Legs." *The New England Journal of Medicine*. Med 1998; 338:1105-1111.

- [13] Chithriki M., Jaibaji M., Steele R. “The anatomical relationship of the aortic bifurcation to the lumbar vertebrae: a MRI study.” *Surgical and Radiologic Anatomy*. Vol. 24,5. p. 308-312. 2002.
- [14] Van de Ven P.J.G., Beutler J.J., Geyskes G.G., Koomans H.A., Kaatee R., Beek F.J.A., Mali W.P.Th.M. “Transluminal vascular stent for ostial atherosclerotic renal artery stenosis.” *The Lancet*. Vol. 346,8976. p. 672-674. 1995.
- [15] Čanić S., et al. “Modeling Viscoelastic Behavior of Arterial Walls and Their Interaction with Pulsatile Blood Flow.” *SLAM Journal on Applied Mathematics*. Vol. 67,1. p. 164-193. 2006.
- [16] National Heart, Lung, and Blood Institute. “The Seventh Report of the Joint National Committee on Prevention, Detection, Evaluation, and Treatment of High Blood Pressure.” *National High Blood Pressure Education Program*. Report No.: 04-5230. 2004.
- [17] Jiang, C. “3D Bifurcating Artery.” *Cornell University: Confluence*. 2014.
- [18] Gabe I.T., Gault J.H., Ross J., Mason D.T., Mills C.J., Schillingford J.P. “Measurement of Instantaneous Blood Flow Velocity and Pressure in Conscious Man with a Catheter-Tip Velocity Probe.” *Circulation*. Vol. 40,5. p. 603-614. 1969.
- [19] Munson, Rothmayer, Okiishi, Huebsch. *Fundamentals of Fluid Mechanics*. 7th ed. Wiley. 2013.
- [20] Dassault Systèmes. “Choosing SOLIDWORKS.” *Dassault Systèmes SolidWorks Corporation*. 2018. Web.
- [21] ANSYS. “Products: Fluent.” *ANSYS, Inc*. 2018. Web.
- [22] Zalger, J.M. “A Fluid-Structure Interaction Analysis of the Human Aortic Arch Under Inertial Load.” *Ryerson University*. Graduate Thesis. 2008.
- [23] Wang S.H. “A linear relation between the compressibility and density of blood.” *The Journal of the Acoustical Society of America*. Vol. 109,1. 2001.
- [24] Groot J.E., Mathai V., Boersen J.T., Sun C., Slump C.H., Goverde P.C.J.M., Versluis M., Reijnen M.M.P.J. “Hemodynamic comparison of stent configurations used for aortoiliac occlusive disease.” *Journal of Vascular Surgery*. Vol. 66,1. p.251-260.e1. 2017.
- [25] LaDisa J.F. Jr., Olson L.E., Guler I., Hettrick D.A., Kersten J.R., Wartier D.C., Pagel P.S. “Circumferential vascular deformation after stent implantation alters wall shear stress evaluated with time-dependent 3D computational fluid dynamics models.” *Journal of Applied Physiology*. Vol. 98,3. p.947-957. 2005.
- [26] Moon J.Y., et al. “The Results of Self-Expandable Kissing Stents in Aortic Bifurcation.” *Vascular Specialist International*. 31.1: 15-19. 2015.

- [27] Panuccio, G. "Performance of Bridging Stent Grafts in Fenestrated and Branched Aortic Endografting." *European Journal of Vascular and Endovascular Surgery*. Vol. 50,1. p.60-70. 2015.
- [28] Kashyap V.S., Pavkov M.L., Bena J.F., Sarac T.P., O'Hara P.J., Lyden S.P, Clair D.G. "The management of severe aortoiliac occlusive disease: Endovascular therapy rivals open reconstruction." *Journal of Vascular Surgery*. Vol. 48,6. p. 1451-1457. 2008.
- [29] Klein W.M. et al. "Dutch iliac stent trial: long-term results in patients randomized for primary or selective stent placement." *Vascular and Interventional Radiology*. Vol. 238,2. p. 734-744. 2006.
- [30] Kandail, H., Hamady, M., Xu, X.Y. "Effect of Flared Renal Stent on the Performance of Fenestrated Stent-Grafts at Rest and Exercise Conditions." *Journal of Endovascular Therapy*. Vol. 23,5. p. 809-820. 2016.
- [31] Scurr J.R.H., McWilliams R.G. "Fenestrated Aortic Stent Grafts." *Seminars in Interventional Radiology*. Open Access. 2007.

Vita

Alexander Joseph Wirtz

Degrees

M.S. Mechanical Engineering, Washington University in St. Louis, May 2018

B.S. Mechanical Engineering, Washington University in St. Louis, May 2017

Summa Cum Laude, Robotics Minor, Mechatronics Minor

B.S. Mathematics-Physics, The College of Idaho, May 2017

Summa Cum Laude, Psychology Minor

Professional Societies

Pi Tau Sigma Mechanical Engineering Honor Society

Sigma Chi Fraternity, Kappa Lambda Chapter